PADME Run-III analysis progress and Run IV physics run status

Tommaso Spadaro* on
behalf of the PADME
collaboration

May 14, 2025

* Laboratori Nazionali di Frascati, INFN tommaso.spadaro@lnf.infn.it

The context

De-excitation of light nuclei via IPC, an anomaly in the decay of ^{8}Be and ^{4}He

$p + A \rightarrow N^\star \rightarrow N + e^+e^-$

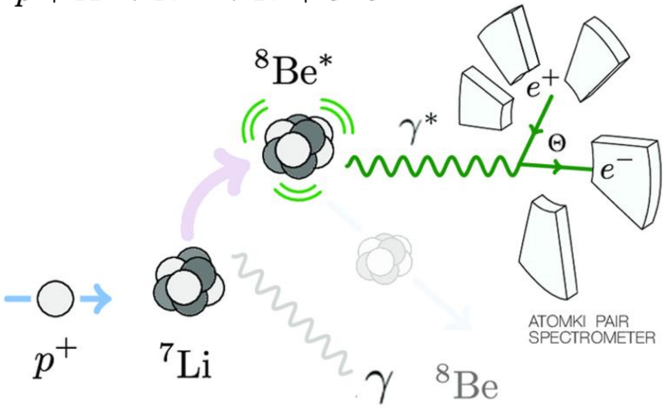

PRL 116, 042501 (2016)

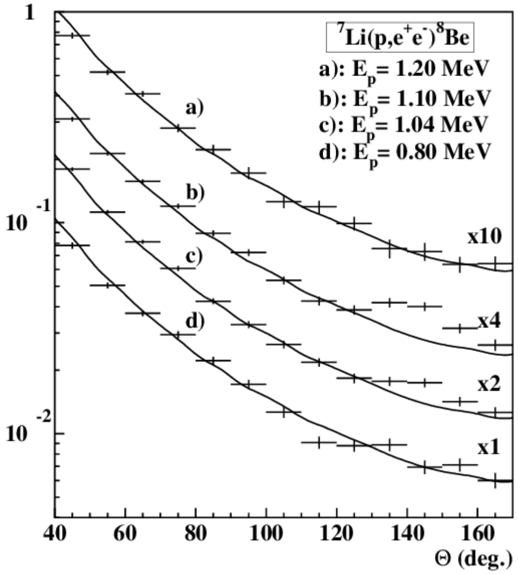

Phys. Rev. C 104, 044003 (2021)

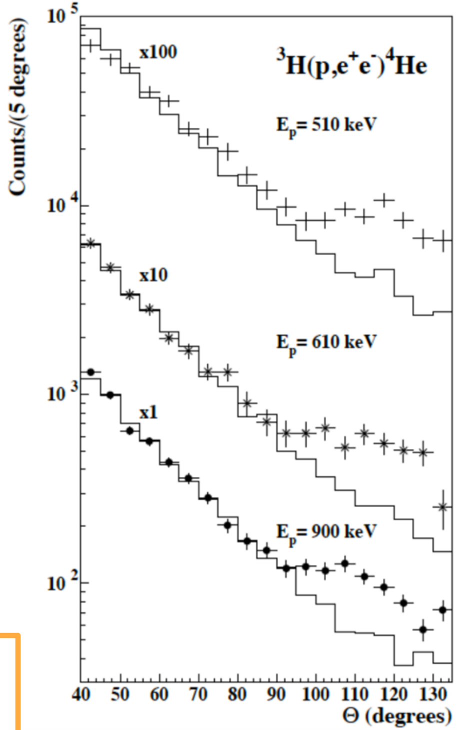

m_χ = (16.98 ± 0.16 ± 0.20) MeV

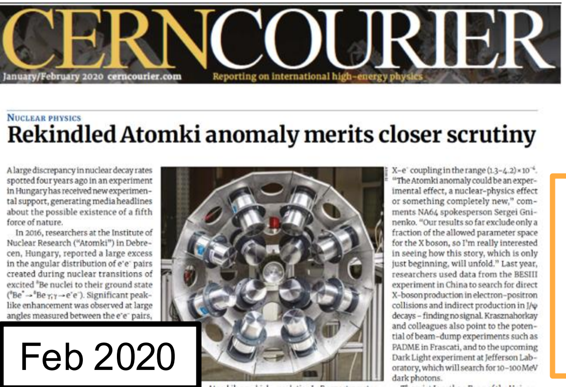
CERNCOURIER

January/February 2020 cerncourier.com Reporting on international high-energy physics

NUCLEAR PHYSICS

Rekindled Atomki anomaly merits closer scrutiny

A large discrepancy in nuclear decay rates spotted four years ago in an experiment in Hungary has received new experimental support, generating media headlines about the possible existence of a fifth force of nature.

In 2016, researchers at the Institute of Nuclear Research ("Atomki") in Debrecen, Hungary, reported a large excess in the angular distribution of e⁺e⁻ pairs created during nuclear transitions of excited ^{8}Be nuclei to their ground state (^{8}Be* → ^{8}Be γ; γ → e⁺e⁻). Significant peak-like enhancement was observed at large angles measured between the e⁺e⁻ pairs,

X–e⁻ coupling in the range (1.3–4.2)×10⁻⁴. "The Atomki anomaly could be an experimental effect, a nuclear-physics effect or something completely new," comments NA64 spokesperson Sergei Gninenko. "Our results so far exclude only a fraction of the allowed parameter space for the X boson, so I'm really interested in seeing how this story, which is only just beginning, will unfold." Last year, researchers used data from the BESIII experiment in China to search for direct X-boson production in electron–positron collisions and indirect production in J/ψ decays – finding no signal. Krasznahorkay and colleagues also point to the potential of beam-dump experiments such as PADME in Frascati, and to the upcoming Dark Light experiment at Jefferson Laboratory, which will search for 10–100 MeV dark photons.

Feb 2020

In ^{12}C [PRC 106, L061601], GDR of ^{8}Be [2308.06473], in ^{8}Be/12C at HUS (Vietnam)

Other efforts ongoing (e-, n beams, etc.)

An update: the MEG-II dedicated measurement

Recent result from MEG II, arXiv:2411.07994 still to be published

- **Measurement on Li7 target to reproduce Be8 ATOMKI result, no signal found**
- **ULs on BR(Be8*→ Be8 ee, anomaly)/BR(Be8* → Be8 γ) for 17.6, 18.1 MeV transitions**

The MEG-II result remains compatible [Barducci, et al. ,HEP 04 (2025) 035] with the ATOMKI combination M_X = 16.85(4) MeV [Denton, Gehrlein PRD108, 015009 (2023)]

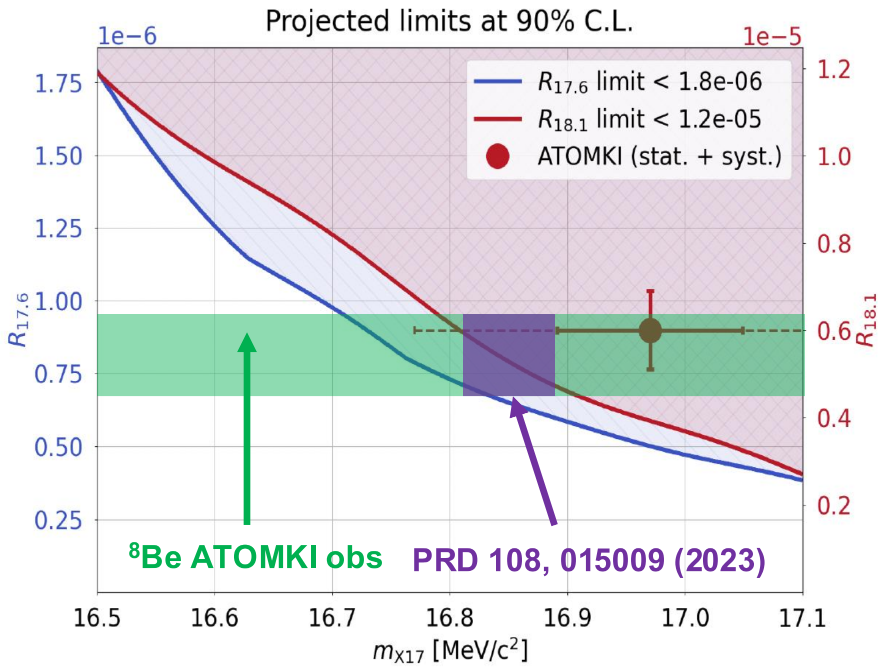

Can PADME help clarifying?

Search for a resonance on a thin target

- $\sigma_{res} \propto \frac{g_{V_e}^2}{2m_e} \pi Z\, \delta(E_{res} - E_{beam})$ **goes with α_{em} → dominant process with respect to alternative signal production processes (α_{em}^2, α_{em}^3)**
- $\sqrt{s}$ **has to be as close as possible to the expected mass → fine scan procedure with the e^+ beam → expected enhancement in $\sqrt{s}$** over the standard model background

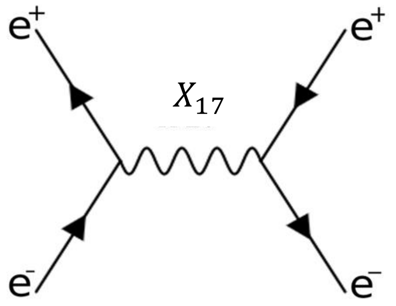

At PADME, X_{17} produced through resonant annihilation in thin target:
Scan around E(e^+) ~ 283 MeV with the aim to measure two-body final state yield N_2

$$N_2(s) = N_{POT}(s) \times [\, B(s) + S(s; M_X, g)\, \varepsilon_S(s)\,]$$

to be compared to $N_2(s) = N_{POT}(s) \times B(s)$

Inputs:

- $N_{POT}(s)$ **number of e+ on target from beam-catcher calorimeter**
- $B(s)$ **background yield expected per POT**
- $S(s; M_X, g)$ **signal production expected per POT for {mass, coupling} = {M_X, g}**
- $\varepsilon_S(s)$ **signal acceptance and selection efficiency**

Search for a resonance on a thin target

- **New physics interpretations** not fully excluded → still some phase-space available
- **Many tensions present anyway [Barducci, et al., JHEP 04 (2025) 035]**
- **In the present talk, for brevity, I will focus on the Vector state**

Vector

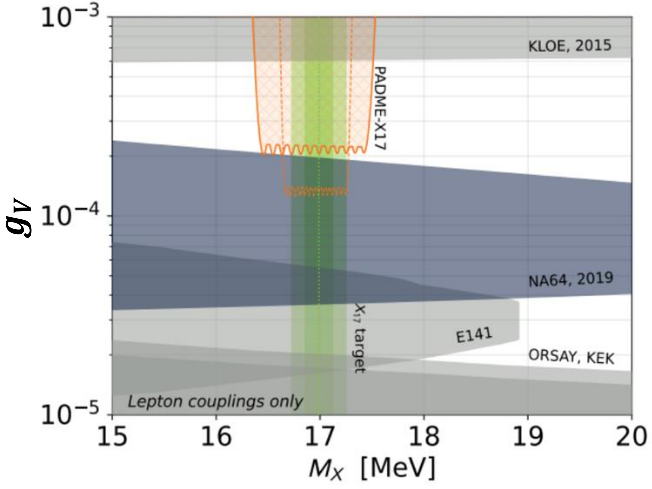

Phys. Rev. D 106, 115036

Pseudoscalar

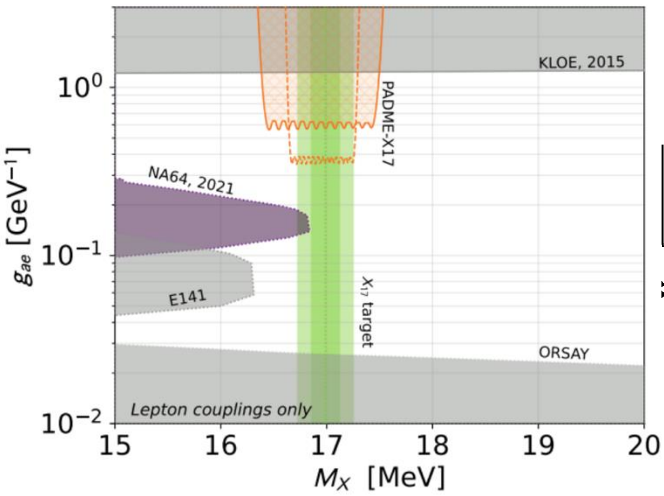

Phys. Rev. D 106, 115036

$$g_{ae} = \frac{V}{m_e}\sqrt{4\pi\alpha_{QED}}$$

What's PADME – the facility

Positrons from the DAFNE LINAC up to 550 MeV, O(0.25%) energy spread

Repetition rate up to 49 Hz, macro bunches of up to 300 ns duration

Intensity must be limited below ~ 3 × 10^4 POT / spill against pile-up

Emittance ~ 1 mm x 1.5 mrad @ PADME

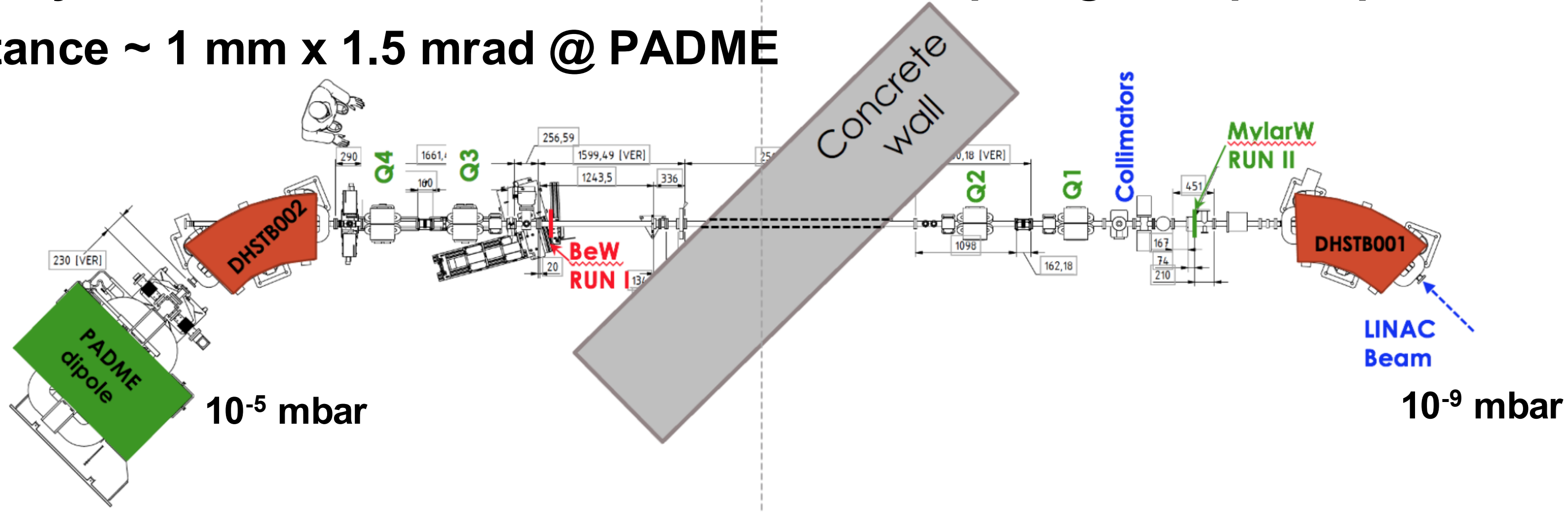

Past operations:

Run I — e^- primary, target, e^+ selection, 250 μm Be vacuum separation [2019]

Run II — e^+ primary beam, 125 μm Mylar™ vacuum separation, 28000 e^+/bunch [2019-20]

Run III — dipole magnet off, ~3000 e^+/bunch, scan $s^{1/2}$ around ~ 17 MeV [End of 2022]

Run-III setup

2022 Run-III setup adapted for the X17 search:

- Active target, polycrystalline diamond
- No magnetic field
- Charged-veto detectors not used
- ECal: 616 BGO crystals, each 21x21x230 mm^3
- Newly built hodoscope in front of Ecal for e/γ
- Timepix silicon-based detector for beam spot
- Lead-glass beam catcher (NA62 LAV spare block)

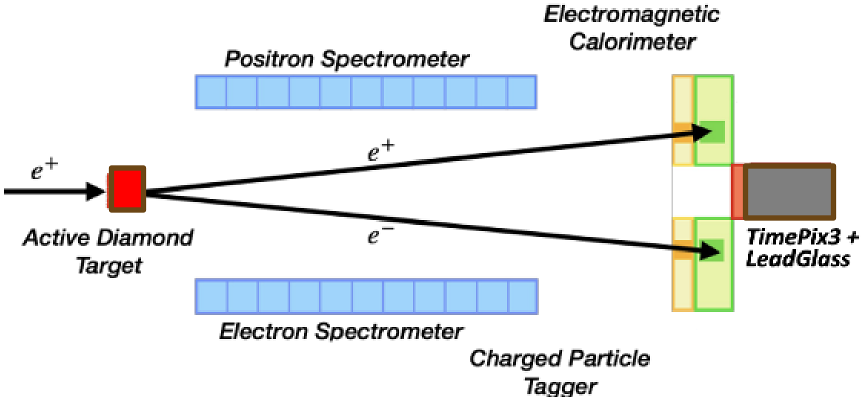

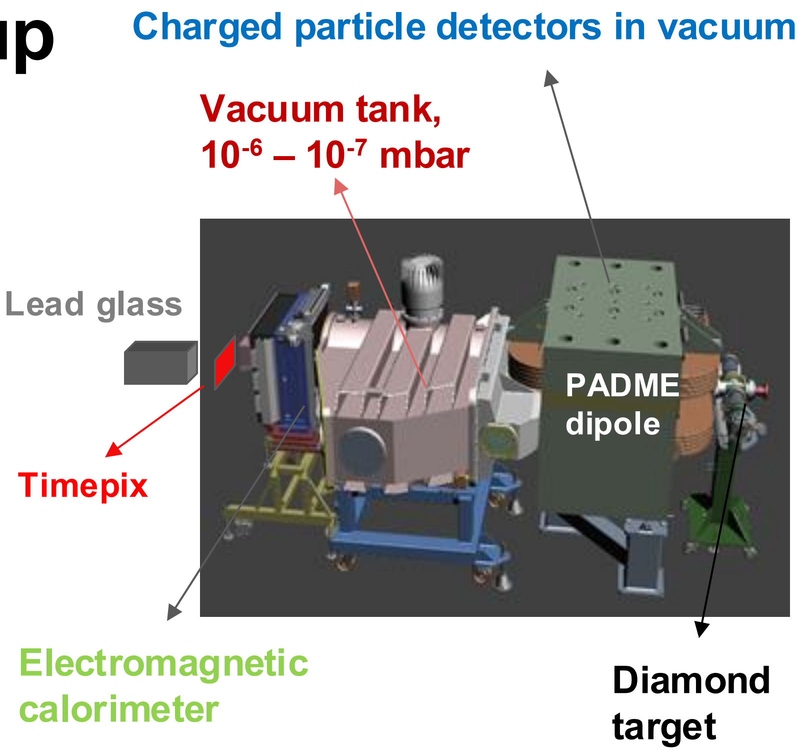

X17 via resonant-production: Run III

Run III PADME data set contains **3 subset**
- **On resonance points (263-299) MeV**
- **Below resonance points (205-211) MeV**
- **Over resonance, energy 402 MeV**

1 over resonance energy point
Statistics ~2 x 10^{10} total
Used to calibrate POT absolute measurement

On resonance points, mass range 16.4 — 17.5 MeV
Beam energy steps ~ 0.75 MeV ~ beam energy spread
Spread equivalent to ~ 20 KeV in mass
Statistics ~ 10^{10} POT per point

Below resonance points
Beam energy steps ~1.5 MeV
Statistics ~ 10^{10} POT per point
Used to cross-check the flux scale

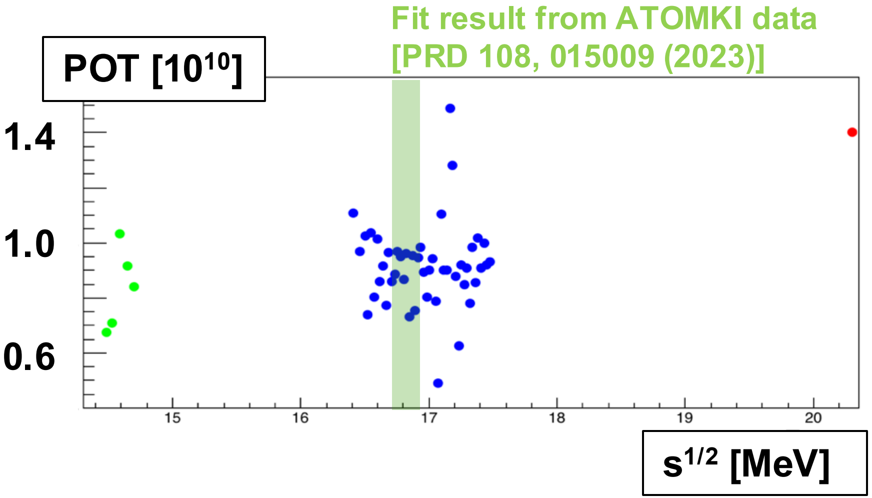

Run-III concepts

"Run": DAQ for ~8 hours, determine beam avg position/angle, ECal energy scale

"Period": a point at a fixed beam energy, typically lasts 24 hours

"Scan" a chronological set of periods typically decreasing in energy

Scan 1 and 2 periods spaced ~ 1.5 MeV but <u>interspersed in energy</u>

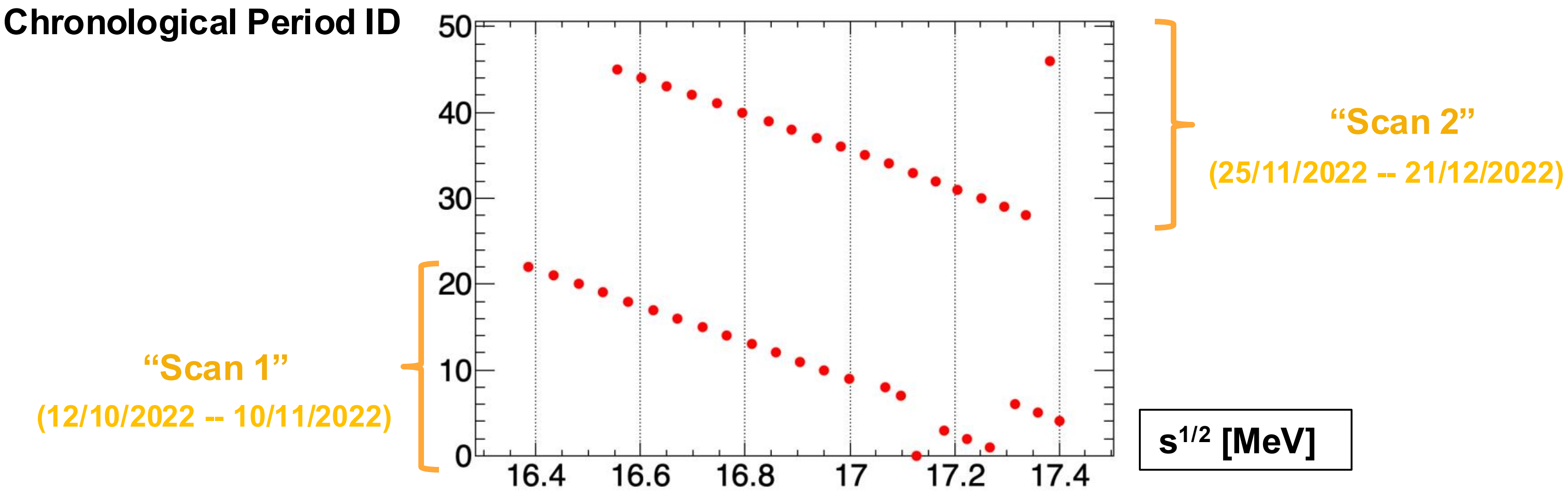

Detailed GEANT4-based MC performed for each period

Run-III concepts – the signal selection

Select any two-body final state (ee, $\gamma\gamma$) with both daughters in ECal acceptance:

1. Fix R_{Max} at Ecal, away from Ecal edges
2. Given s, derive R_{Min}, E_{Min}, E_{Max}
3. Select cluster pairs:
   - With Energy > E_{min} x 0.4
   - In time within 5 ns
   - Clus1: In (R_{min}- D, R_{max}), D = 1.5 L3 crystals
   - Clus2: R > R_{min}- D
4. Select pairs back-to-back in the c.m. frame

Rmax chosen to be away from Ecal edges by more than the size of 1 L3 crystal cell for any period in the data set

1 □ = 1 L3 crystal = 21.5 x 21.5 mm

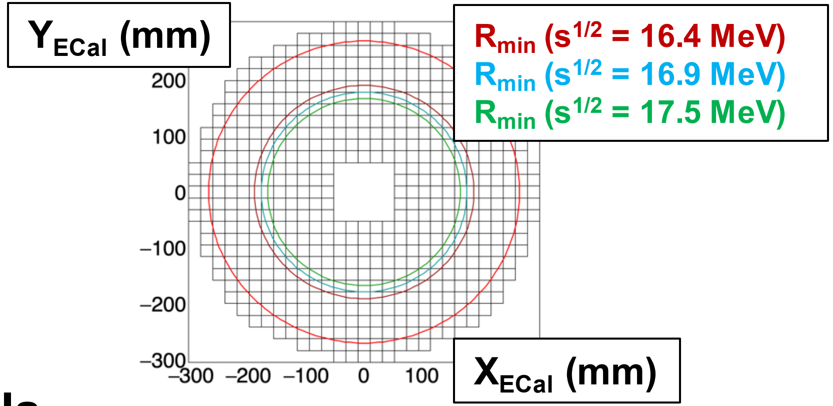

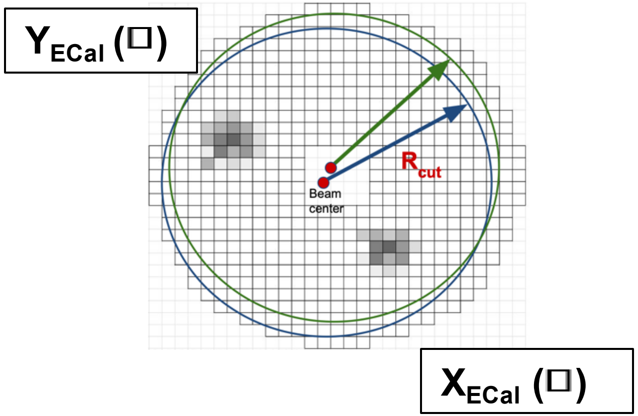

Run-III concepts – the signal selection

Neglecting m_e/E terms, the c.m. angles are independent on the lab energies

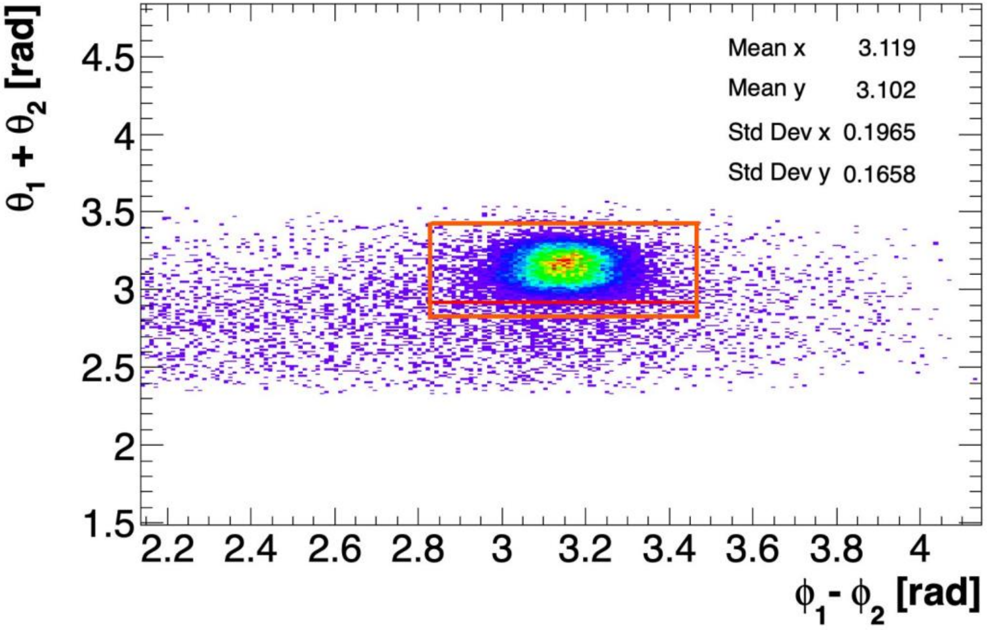

Selection region

Sideband region

Run-III concepts – the signal selection

Selection algorithm made as independent as possible on the beam variations:

- **Retune beam center run by run with an error << mm**
- **Overall, make marginal use of the cluster reconstructed energy**

Selected events, 4 % background

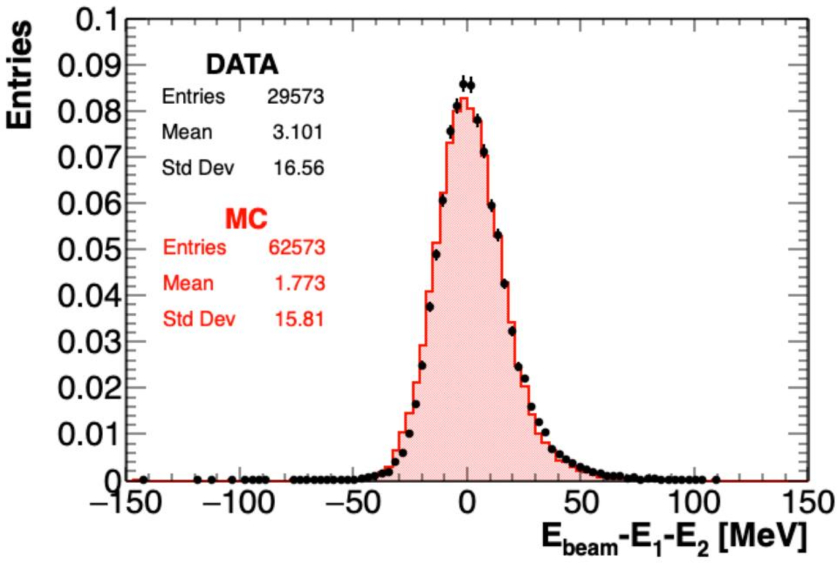

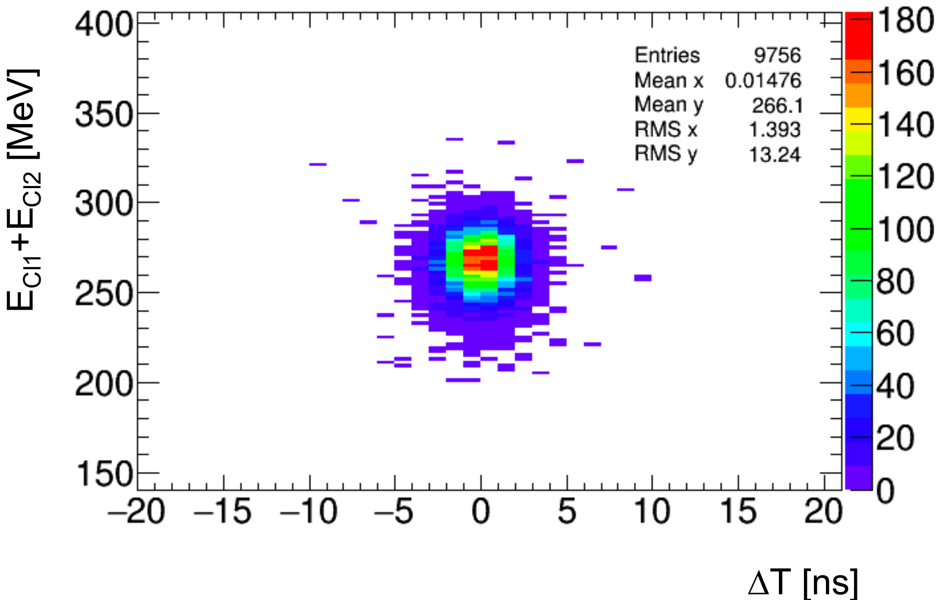

Grand scheme of the analysis

Rewrite the master formula as:

$$\underbrace{N_2(s) / (N_{POT}(s)\ B(s))}_{g_R(s)} = [1 + S(s; M_X, g)\ \varepsilon_S(s) / B(s)]$$

The analysis observable is $g_R(s)$

Different effects (see later) lead to a linear scale deviation K(s) from above

Question: is $g_R(s)$ more consistent with
- **K(s) or with**
- **K(s) $[1 + S(s; M_X, g)\ \varepsilon_S / B]$?**

MC with M_X = 16.8 MeV, $g_V = 8 \times 10^{-4}$

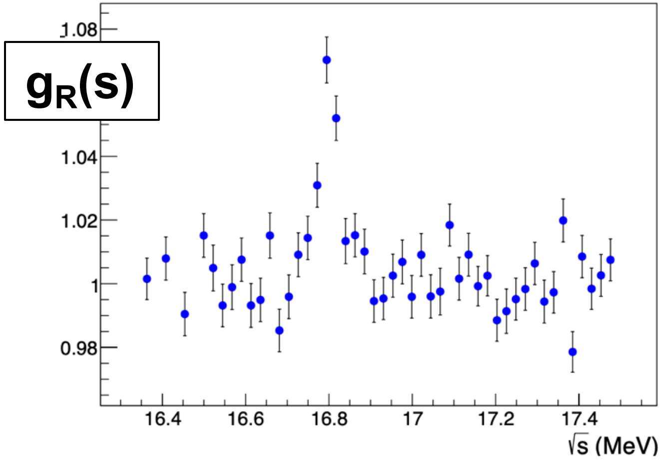

The N_2 event yield error budget

Selection counts around 30k / period:

Statistical error: δN_2 ~ 0.6% up to 0.7%

Background subtraction using angular side-bands (bremsstrahlung, 4%)

Carries additional statistical uncertainty δN_2 ~ 0.3%

Data quality using time-averaged energy deposited on ECal:

Dominated by primary beam (brems. on upstream vacuum separation window)
Contribution of two-body events negligible
A few % of the spills are outliers and removed
Overall systematic error from data quality, $\delta N_2 << \%$

Source	Error on N_2 per period [%]
Statistics	~0.6
Background subtraction	0.3
Total	0.65

Grand analysis scheme: B

B , the expected background / e^+, is determined with MC + data-driven checks

Source	Error on B per period [%]	Details
MC statistics	0.4	Next slide
Data/MC efficiency (Tag&Probe)	0.3	here
Cut stability	0.2	here
Beam spot variations	0.1	here
Total	0.55	

Correlated (common) systematic errors on B enter in the scale K(s), e.g.:

Absolute cross section (rad. corr. at 3%), target thickness (known @ 5%)

B expectation is compared to below resonance points, improving the systematic uncertainty

Scaling errors are accounted for

Source	Correlated B error [%]	Details
Low-energy period statistics	0.4	
Acceptance of low-energy, target thickness variations	1.0	here
Total	1.1	

Details on expected background: s dependence

Expected background B determined from MC, stat error per period: $\delta B \sim 4\times10^{-3}$

Fit of $B(s^{1/2})$ with a straight line (only including statistical errors here)

B [10^{-6} events per POT]

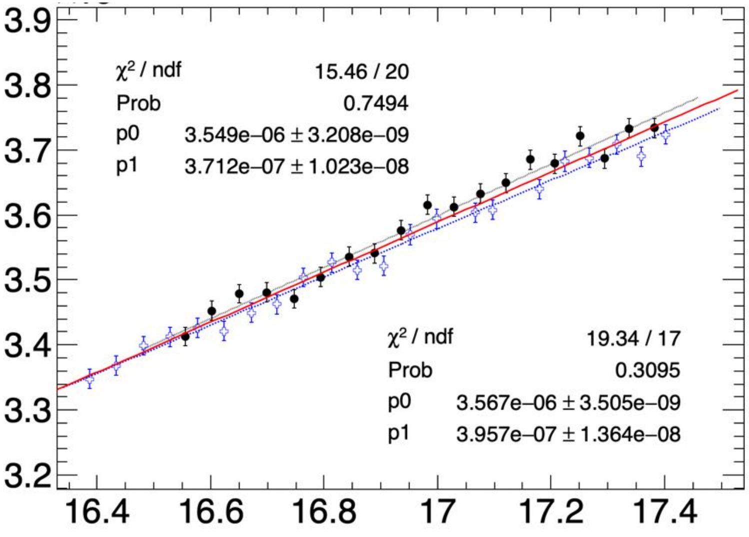

$s^{1/2}$ (MeV)

Fit mode	P0 [10^{-6}]	P1 [10^{-7} / MeV]	Corr	Fit prob
Only scan1	3.549(3)	3.71(10)	0.12	75%
Only scan2	3.567(4)	3.96(13)	-0.19	31%
All periods	3.558(2)	3.85(8)	-0.008	9%

Background curve slightly depend on the scan

Considered in alternative analysis (see later)

Grand analysis scheme: N_{POT}

Flux N_{POT} determined using Lead-glass detector charge, Q_{LG}:

$$N_{POT} = Q_{LG} / Q_{1e+,\ 402\ MeV} \times 402 / E_{beam}\ [MeV]$$

Common systematic error dominated by Q_{1e+}

Known at 2%, see *JHEP* 08 (2024) 121

Uncorrelated systematic error due to value of E_{beam} from BES, 0.25%

Common scale error on beam energy, up to 0.5%, cancels @ 0.1%

Multiple corrections to be applied:

1. Energy-loss @ E_{beam} / @ 402 MeV: from data + MC, details here
2. Radiation-induced response loss: from data, details here

Grand analysis scheme: N_{POT} error budget

Uncorrelated uncertainty on background N_{POT} :

Source	Error on N_{POT} per point [%]	Source
Statistics, ped subtraction	negligible	
Energy scale from BES	0.3	BES from timepix spot σ_x
Error from rad. induce slope	Variable, ~0.35	here
Total	0.45	

Correlated (common) systematic errors on N_{POT}:

Source	Common error on N_{POT} [%]	Source
pC / MeV	2.0	Analysis in *JHEP* 08 (2024) 121
Energy loss, data/MC	0.5	here
Rad. induced loss, constant term	0.3	here
Total	2.1	

Grand analysis scheme: g_R error budget

Uncorrelated uncertainty on $g_R(s) = N_2(s) / (N_{POT}(s)\ B(s))$:

Relative error per period

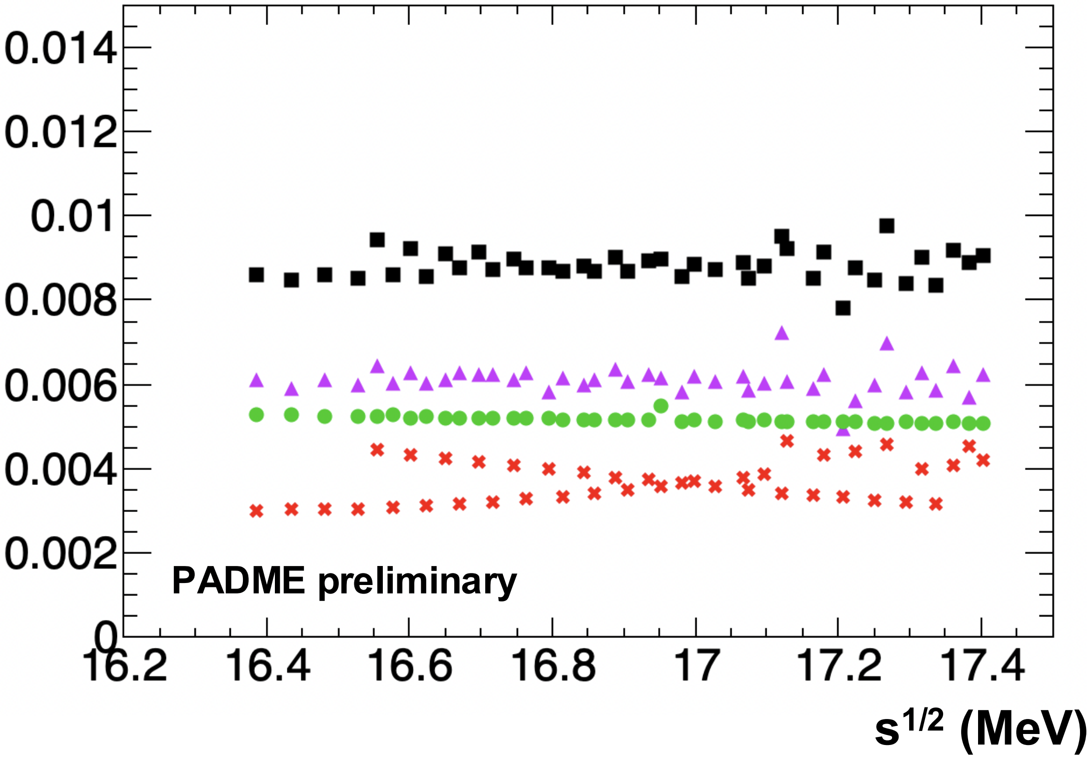

Grand analysis scheme: signal yield / POT, S

Analysis compares $g_R(s)$ to $K(s) \times [1 + S(s; M, g_v)\ \varepsilon/B]$

Expected signal yield from PRL 132 (2024) 261801, includes effect of motion of the atomic electrons in the diamond target from Compton profiles

Parameterized S vs E_{beam} with a Voigt function:

- Convolution of the gaussian BES with the Lorentzian
- OK in the core within % with some dependence on BES

Uncertainty in the curve parameters as nuisances:

- Peak yield: 1.3%
- Lorentzian width around the resonance energy: 1.72(4) MeV
- Relative BES, as said: 0.025(5)%

$S(E_{beam}; M_X = 17\ \text{MeV}, g_v = 10^{-3})$

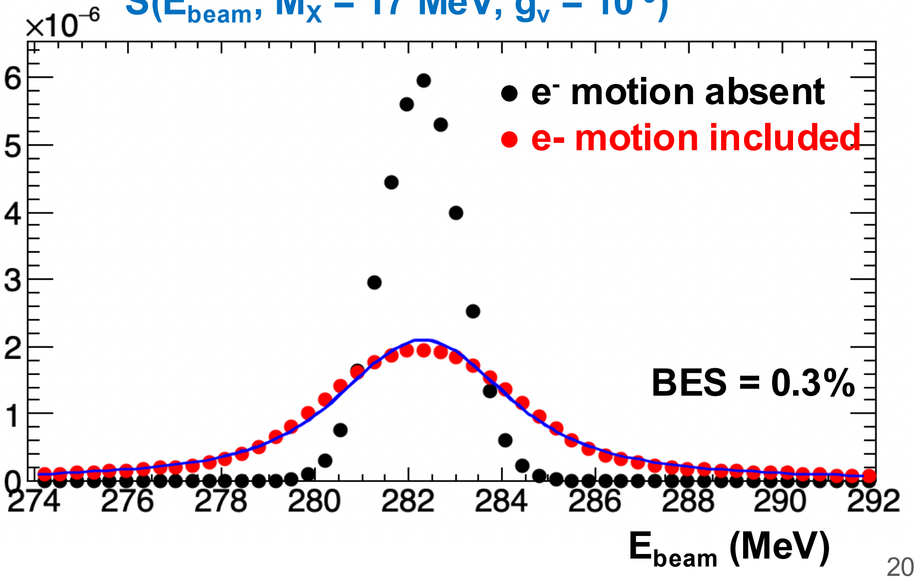

Points from authors of PRL 132 (2024) 261801

Grand analysis scheme: ε/B

Analysis compares $g_R(s) = N_2 / (B \times N_{POT})$ to $K(s)\ [1 + S(M,g_v)\ \varepsilon/B]$

Expected background signal efficiency ε determined from MC:

- Beam spot vs run from COG, negligible uncertainty from COG error
- Large cancellation of systematic errors seen using ε/B

Fit $\varepsilon/B(s^{1/2})$ with a straight line, include fit parameters as nuisances:

- Errors: $\delta P0/P0 \sim 0.1\%$, $\delta P1/P1 = 3\%$, correlation = -2.5%
- Separate fits for scan1 and 2, basically compatible
- Behavior reproduced with toy MC

Grand analysis scheme: possible scale effects, K(s)

Radiative corrections evaluated using Babayaga, ee(γ) and γγ(γ)

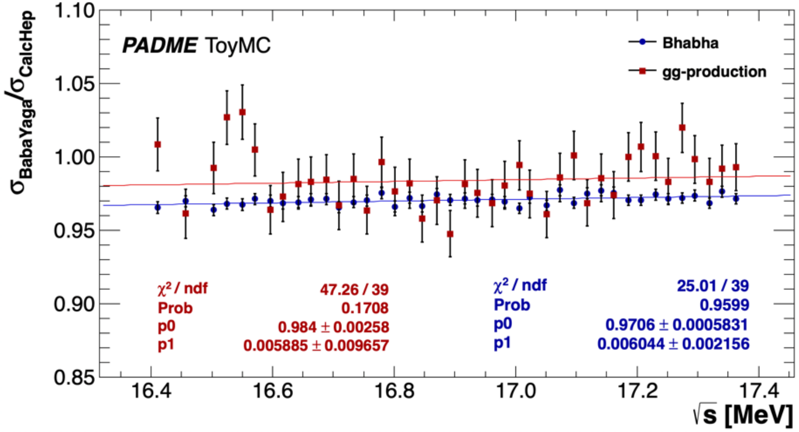

Babayaga references:

Nucl. Phys. B 758 (2006) 227

Phys. Lett B 663 (2008) 209

Possible offset ~ -2.3% @ 16.92 MeV

Possible slope with $s^{1/2}$: -0.6(2)% MeV^{-1}

The scaling with the below resonance is affected by a -1.5(5)% shift because of radiative correction, but the expected total error covers for it: 1.1%(B) + 2.1%(N_{PoT}) = 2.4%

Grand analysis scheme: expected sensitivity

- Evaluate expected 90% CL UL in absence of signal
- Define Q statistic based on Likelihood ratio: $Q = L_{S+B}(g_v, M_X) / L_B$
- The likelihood includes terms for each nuisance parameter pdf
- For a given M_X, $CLs = P_S / (1 - P_B)$ is used to define the UL on g_v

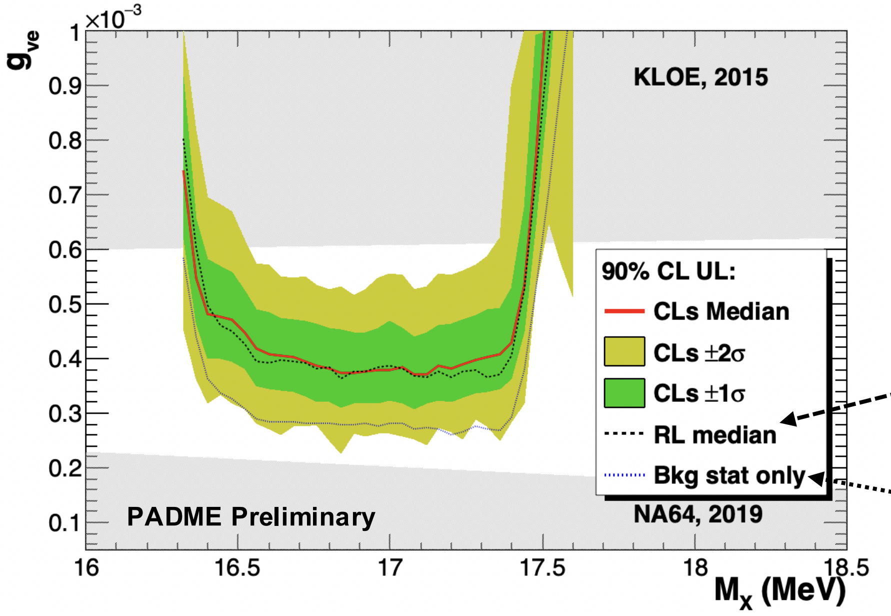

The probabilities P_S and P_B are obtained using simulations, where the observables are always sampled, while the nuisance parameters stick to the B and S+B fits ("θ hat")

For comparison, we show also:

- the median of the limits obtained using the Rolke-Lopez likelihood-ranking method with the 5 periods with largest signal yield
- the purely statistical UL, $1.28\ N_2^{1/2}$

For details, arXiv:2503.05650

Comparison with previous PADME evaluation

Source	Uncertainty [%]		Note
	arXiv:2503.05650	Run-III	
N_2	0.55	0.6	Uncorrelated
N_{PoT}	1.0	0.35	Uncorrelated
B	0.6	0.55	Uncorrelated
Total on g_R	1.29	0.89	Uncorrelated
K(s) scale	2.0	2.4	Common

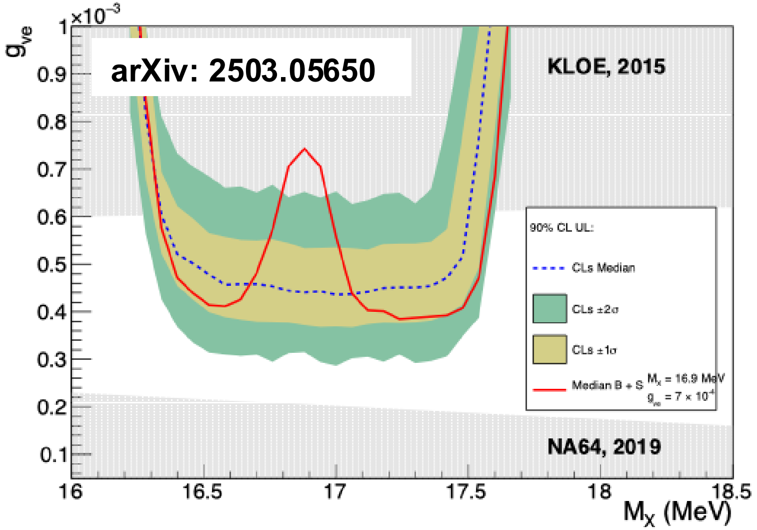

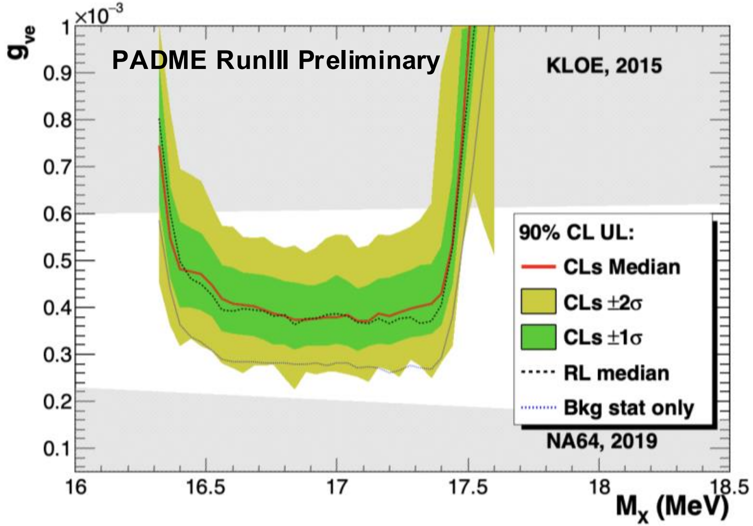

The "blind unblinding" procedure

To validate the error estimate, we applied the procedure in 2503.05650 [hep-ex]

Aim to blindly define a side-band in $g_R(s)$, excluding 10 periods of the scan

Define the masked periods by optimizing the probability of a linear fit in $s^{1/2}$

1. Threshold on the χ^2 fit in side-band is $P(\chi^2)$ = 20%, corresponding to reject 10% of the times
2. If passed, check if the fit pulls are gaussian
3. If passed, check if a straight-line fit of the pulls has no slope in $s^{1/2}$ (within 2 sigma)
4. If passed, check if constant term and slope of the linear fit for K(s) are within two sigma of the expectations, i.e.: +/- 4% for the constant, +-2% MeV^{-1} for the slope

Successfully applied:

1. $P(\chi^2)$ = 74%
2. Pulls gaussian fit probability 60%
3. Slope of pulls consistent with zero
4. Constant term = 1.0116(16), Slope = (-0.010 +- 0.005) MeV^{-1}

Therefore, proceed to box opening

Box opening

Some excess is observed beyond the 2σ local coverage (2.5 σ local)

At M_X = 16.90(2) MeV, g_{ve} = 5.6 x 10^{-4}, the global probability dip reaches $3.9_{-1.1}^{+1.5}$ %, corresponding to (1.77 +- 0.15) σ one-sided (look-elsewhere calculated exactly from the toy pseudo-events)

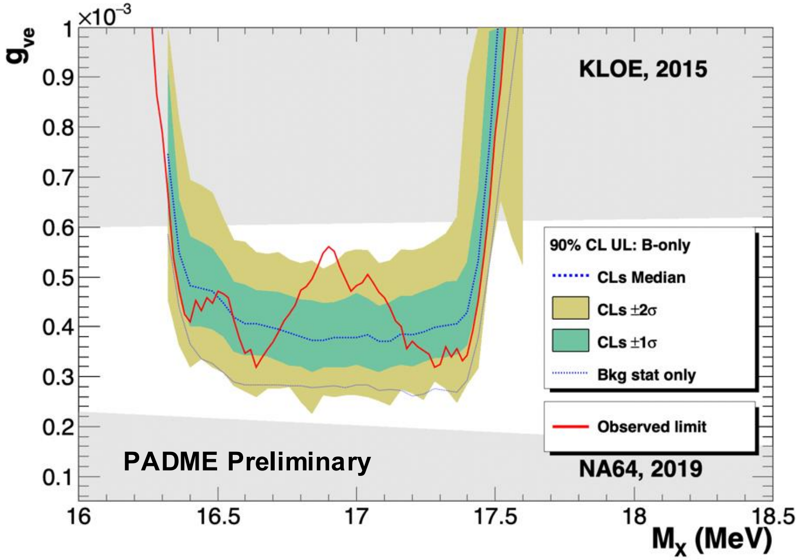

A second excess is present at larger masses ~ 17.1 MeV, but the absolute probability there is ~ 40%

If a 3σ interval is assumed for observation following the estimate M_X = 16.85(4) of PRD 108, 015009 (2023), the p-value dip deepens to $2.2_{-0.8}^{+1.2}$% corresponding to (2.0+-0.2) σ one-sided

Pvalue

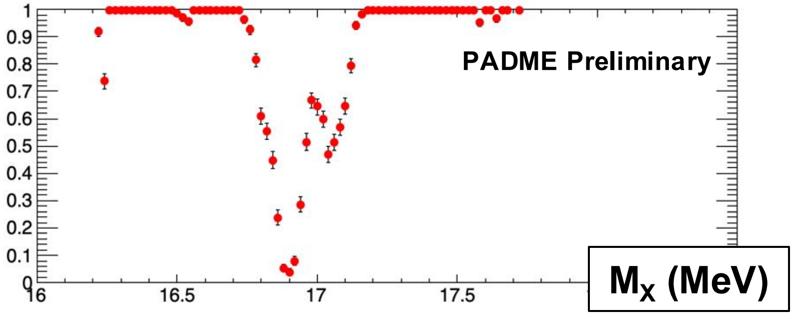

Box opening - II

Check the data distribution vs likelihood fit done to evaluate $Q_{obs}(S+B)$
Fit probability is 60%

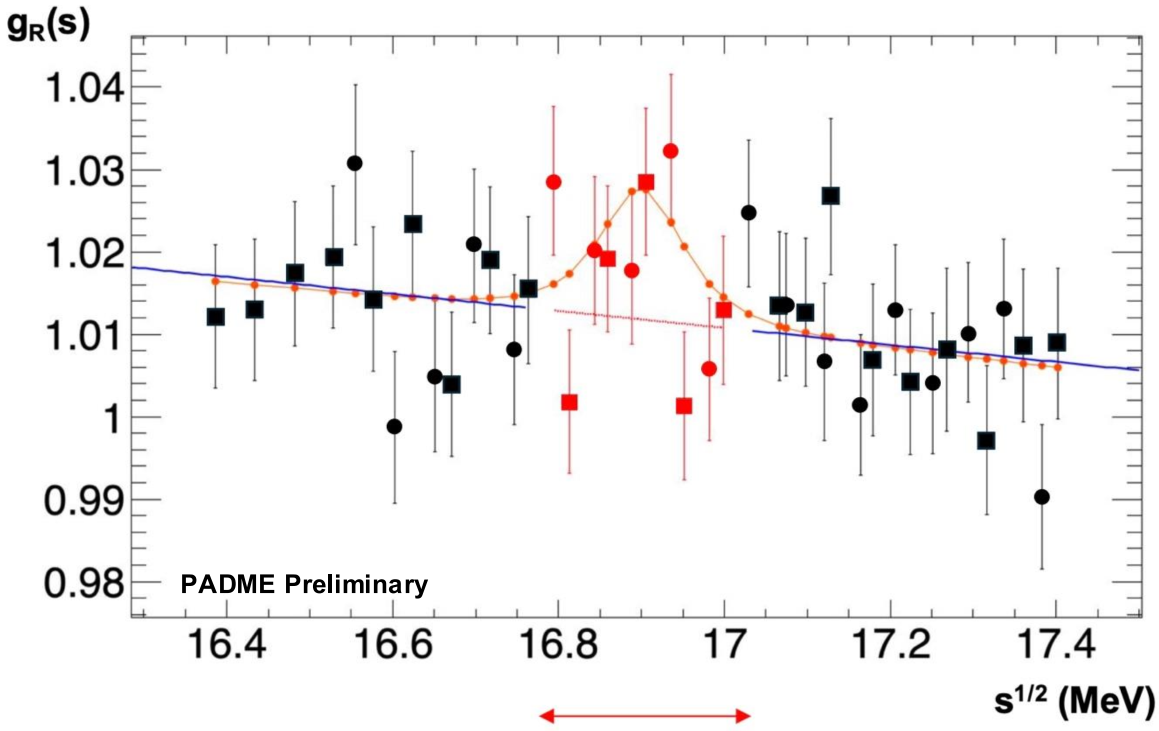

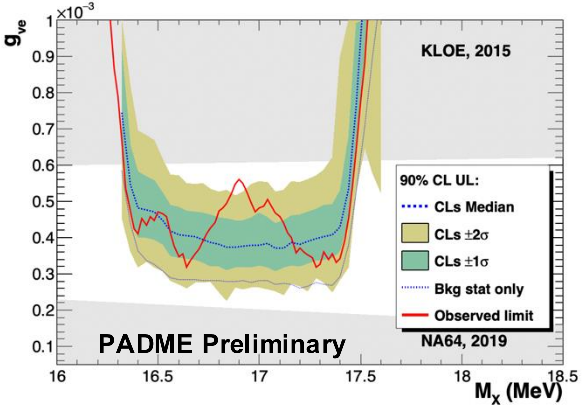

Masked point of scan 1
Masked point of scan 2
Sideband point of scan 1
Sideband point of scan 2

Region masked by automatic procedure

Box opening – II – UL comparison

For comparison, check expected UL bands: bkg-only vs B+S(16.9 MeV, 5 × 10^{-4})

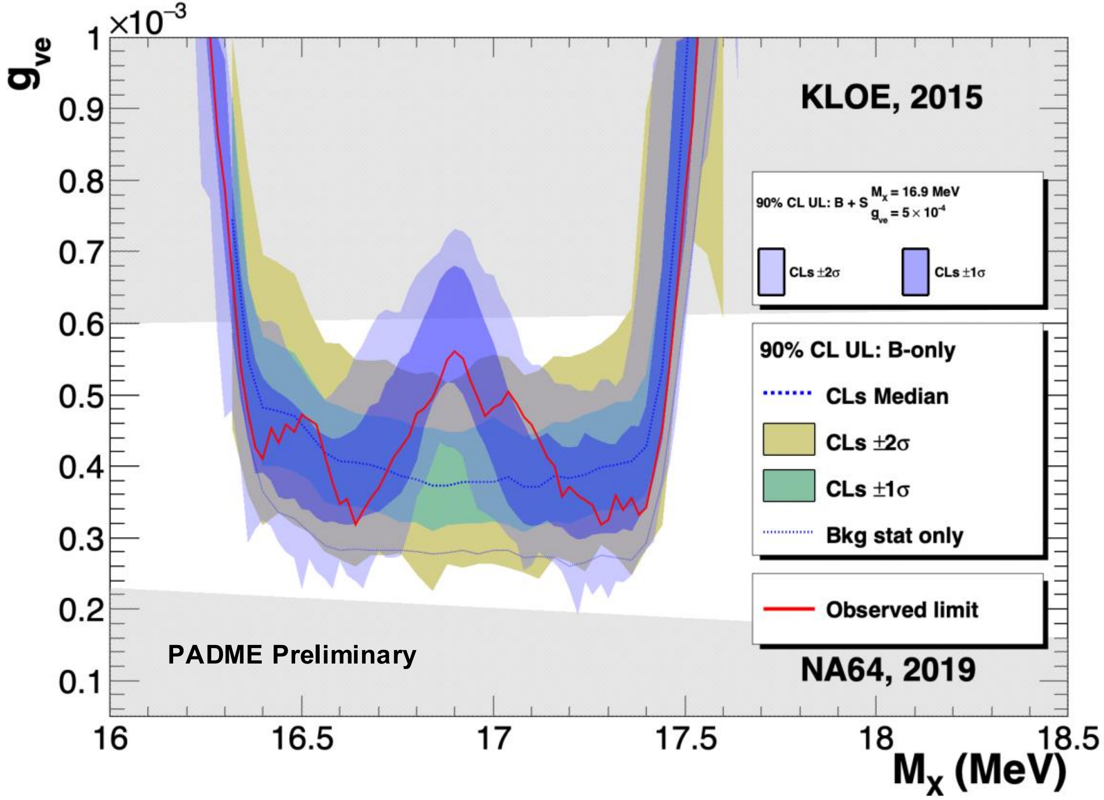

Box opening – III Other checks

Checked other sensitivity methods

Perform the automatic procedure but fit with a constant:

Result:	Original version:
1. $P(\chi^2) = 37\%$	1. $P(\chi^2) = 74\%$
2. Pulls gaussian fit prob > 30%	2. Pulls gaussian fit probability > 45%
3. Slope of pulls consistent with zero	3. Slope of pulls consistent with zero
4. Constant = 1.0112(14)	4. Constant = 1.0116(16), Slope = (-0.010 +- 0.004) MeV^{-1}

The center of the masked region does not change: 16.888 MeV
The excess also remains basically of the same strength: 1.6σ

Use scan1-scan2 separate parametrizations for B(s) instead of using B(s) / point:
The excess region is slightly affected and is equivalent to ~1.6 σ

Check the PCL method using CLsb, equivalent number of σ = 1.62 +- 0.13

Box opening – IV Check of corrections

Checked behavior of $g_R(s)$ for each of the corrections applied: subtraction of background from N_2

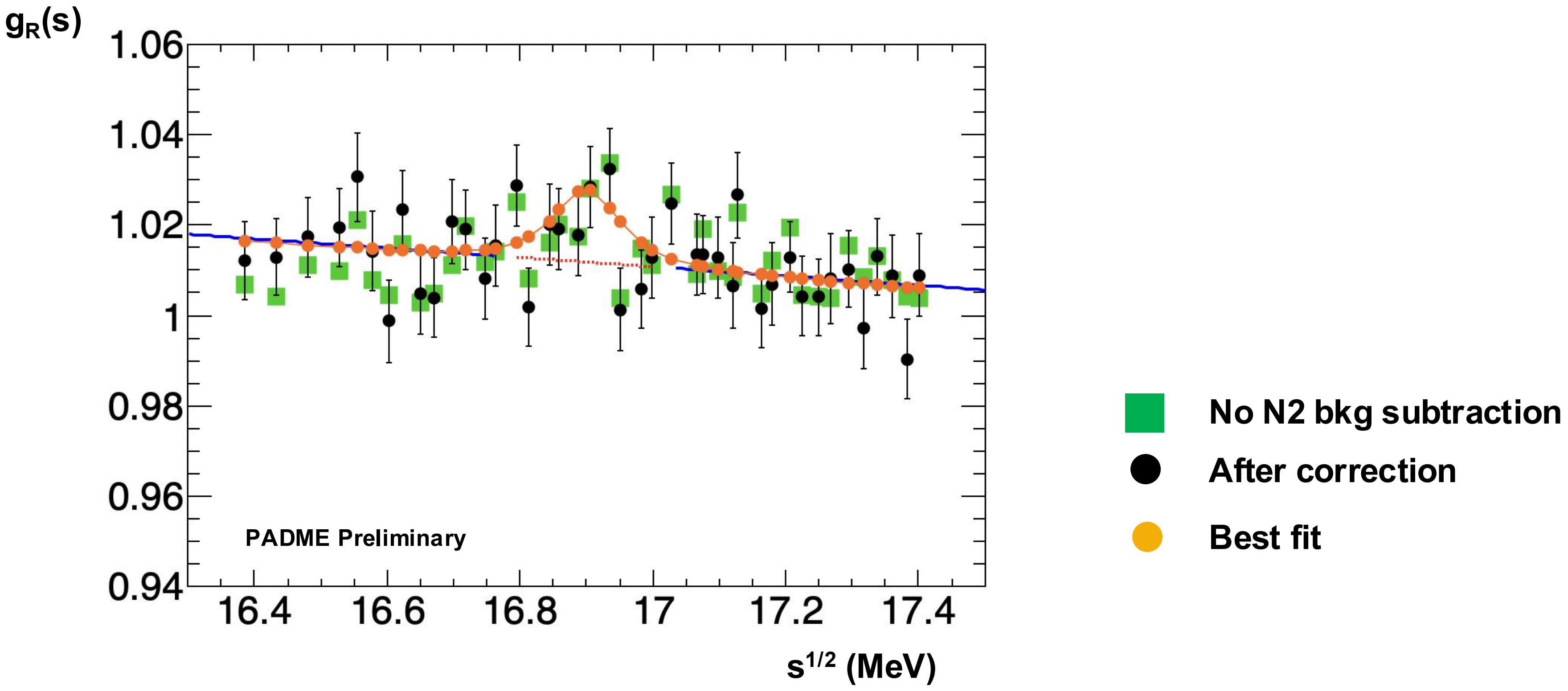

Box opening – IV Check of corrections

Checked behavior of $g_R(s)$ for each of the corrections applied:
leakage correction for NPoT

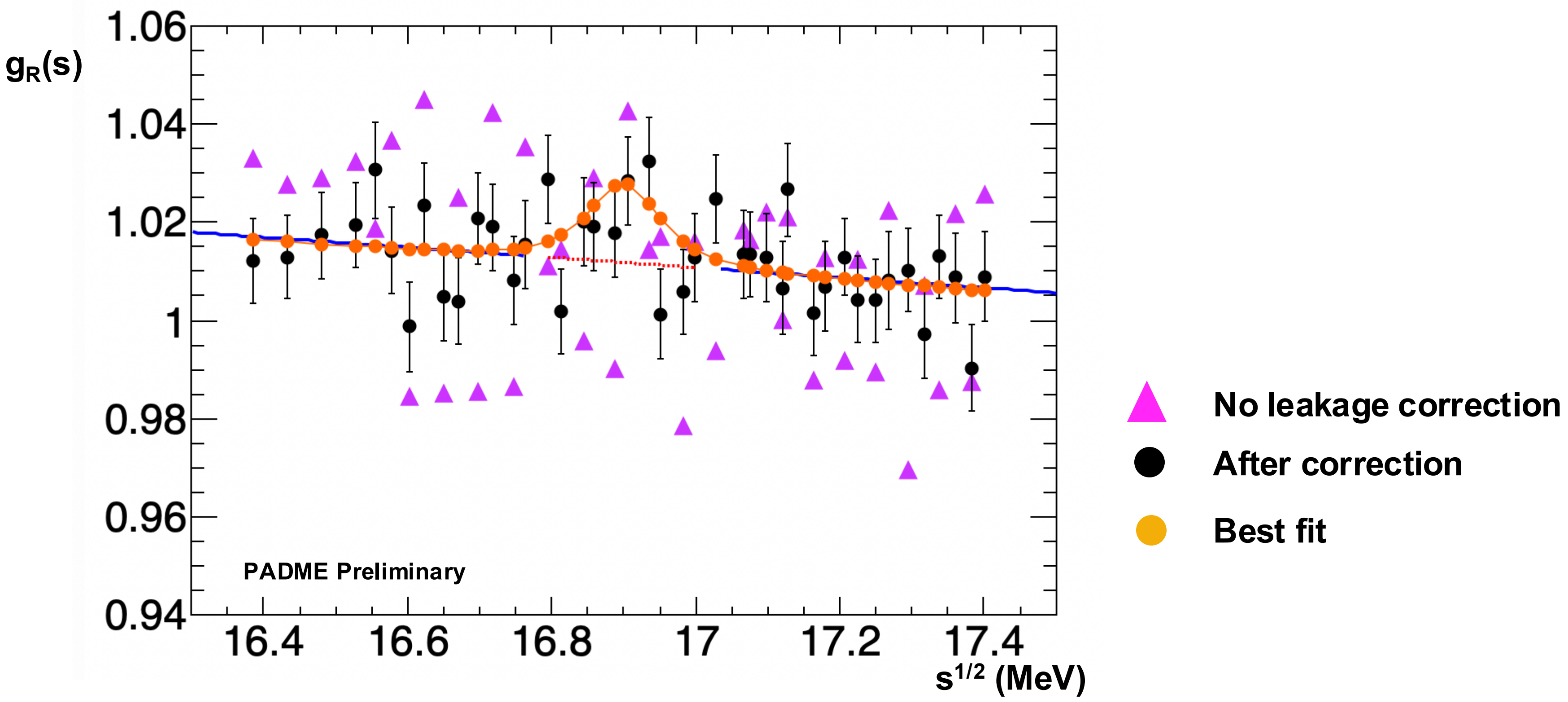

Box opening – IV Check of corrections

Checked behavior of $g_R(s)$ for each of the corrections applied: ageing correction for NPoT

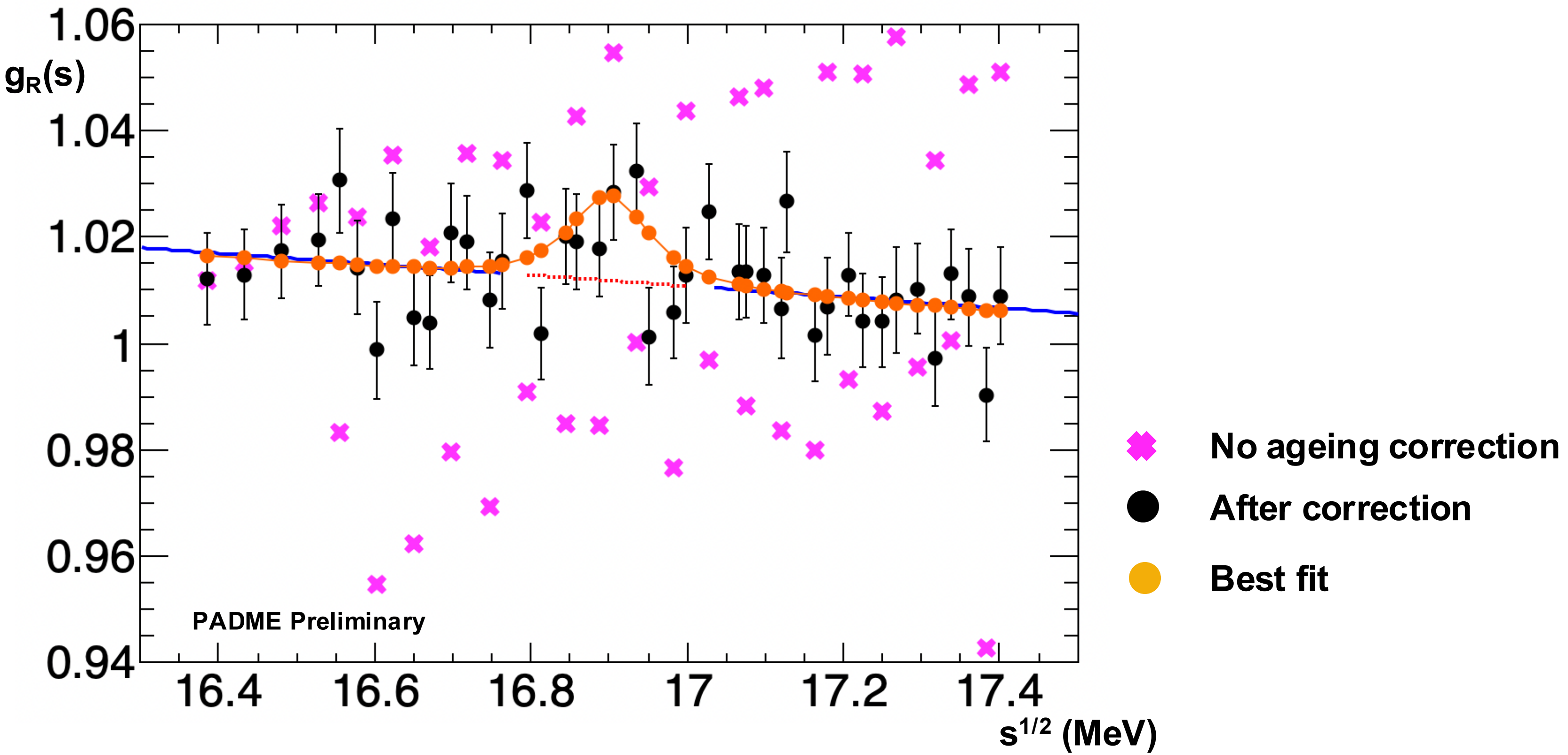

Box opening – IV Check of corrections

After box opening, can check ageing correction applied, slope was 0.097(7)
Fully consistent (observed excess alters only marginally)

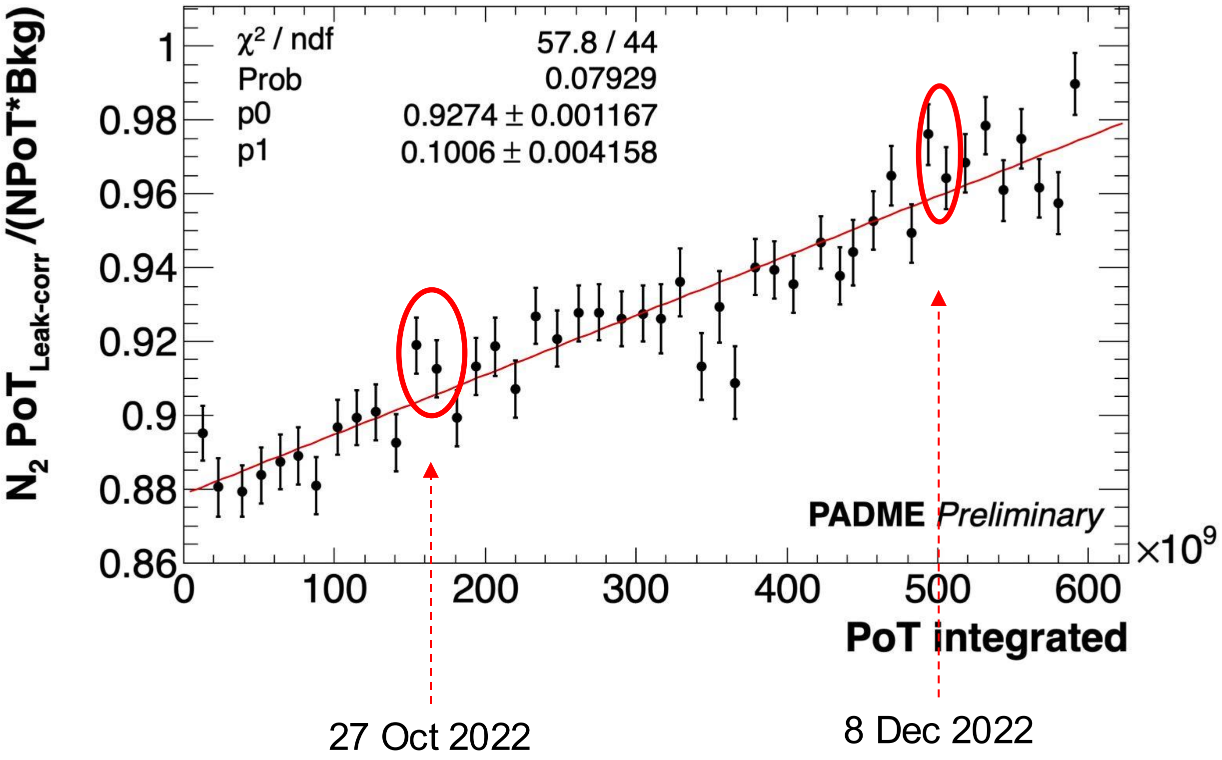

Conclusions (I) – Run III result

The analysis has been successfully blessed using the blind-sideband method

Overall uncertainties at 0.9% or slightly better

No indications of X17 well beyond two-sigma-equivalent global p-values

An excess has been observed, with global p-value equivalent to 1.77(15) σ

Nothing of what I have shown would have been possible without the relentless effort of our colleagues of the accelerator division and particularly the LINAC and BTF teams and the vacuum and mechanical engineering service. We would also like to thank the contribution of all the services of the research division (servizio progettazione, servizio supporto esperimenti, servizio elettronica). We acknowledge also the valuable contributions of the technical division and the administrative service

Run IV – optimized setup

New data set to be acquired to better clarify:

- **set the target closer to the Ecal, increase acceptance by x2**
- **possible with a new support for motor actuator (and zero magnetic field)**

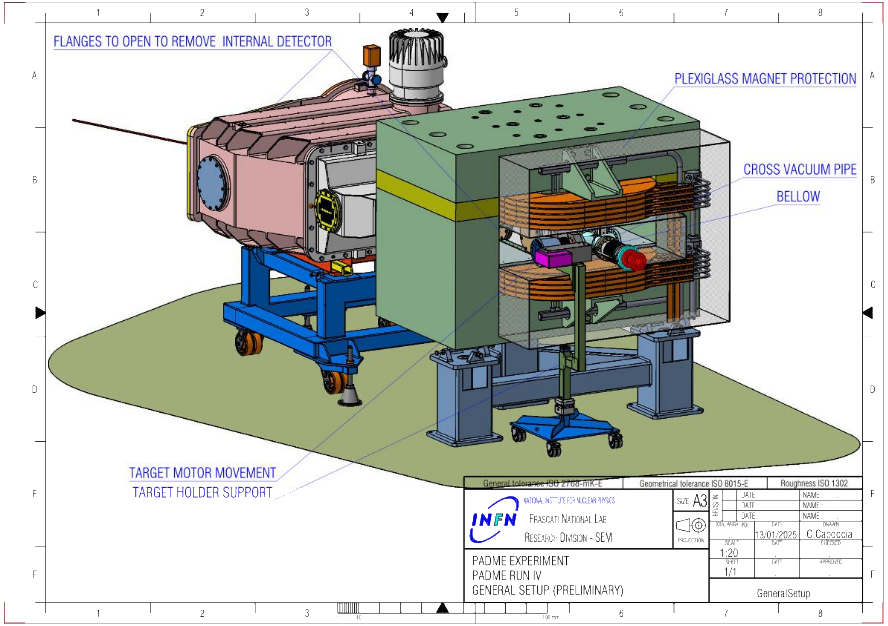

Activity concluded in February, vacuum started beginning of March

Run IV – new tracking detector

A new detector for Run IV:

- **micromegas-based tracker to separately measure the absolute cross sections of ee/γγ thus allowing a combined analysis**
- **Huge improvement in measurement of angles, also provides beam spot**

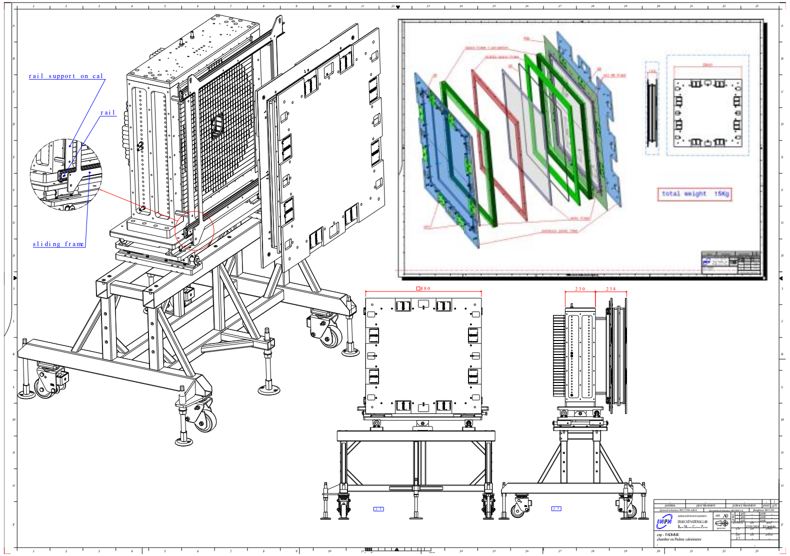

Two 5 cm gaps, can operate in TPC mode

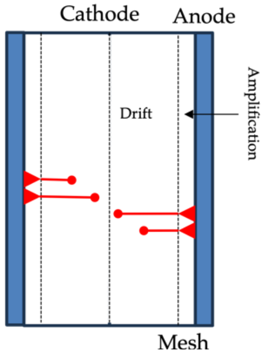

Resistive circuit (common, 3HV zones)

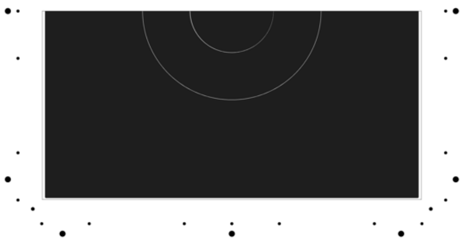

Installed 31 March, thanks to the new experts participating from LNF, Roma1, Neaples INFN sections

Run IV assumptions

Assumptions for Run IV:
- **x2 acceptance increase (target closer to ECal)**
- **x2 statistics increase, 1.5×10^{10} POT per energy point**

Assume to acquire 2 points / week:
- **1 day for beam optimization and tuning**
- **2.5 days for data collection, 3000 e^{+} / spill as in Run III**

Points divided into 2 scans:
- **16—20 points per scan**
- **1 scan in 8—10 weeks**

Acquiring each scan in a continuous data taking period is strongly preferable

Run IV projections

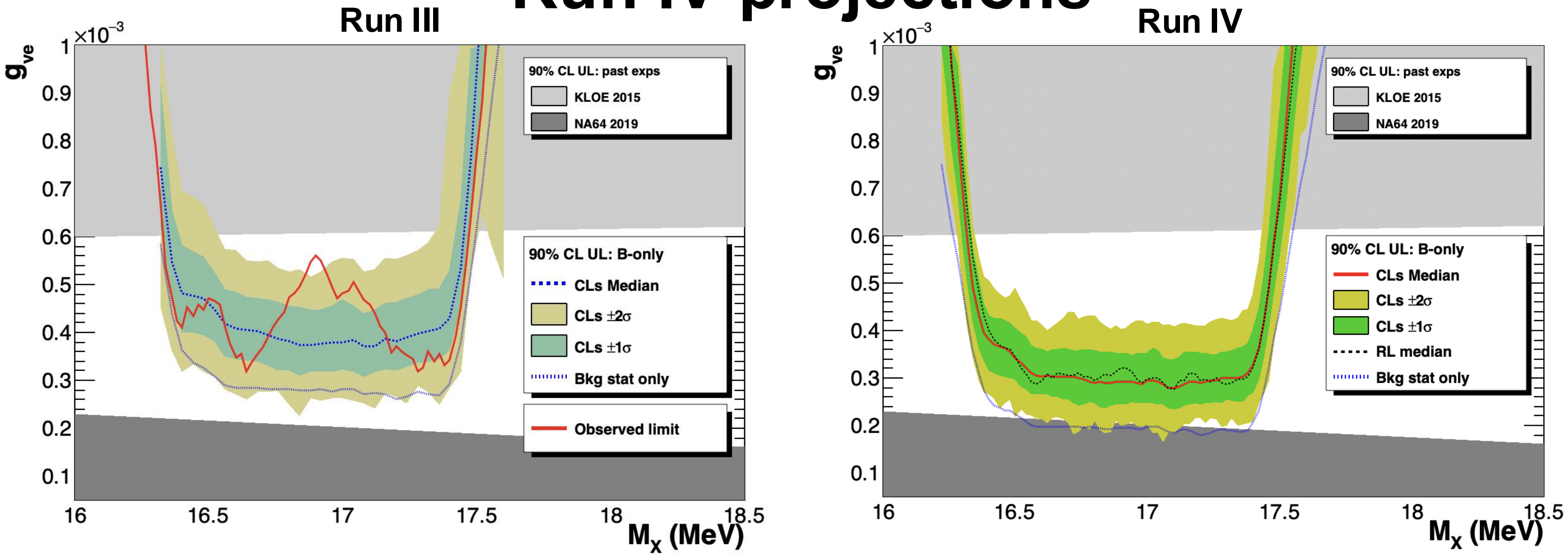

Source	Uncertainty [%]		Note
	Run III	Run IV	
N_2	0.6	0.3	Uncorrelated
N_{PoT}	0.35	0.3	Uncorrelated
B	0.55	0.3	Uncorrelated
Total on g_R	0.89	0.5	Uncorrelated

Conclusions (II) – Run IV perspectives

Run III has been successful: uncertainty better than 1% on 40+ points

Lessons for Run IV to improve:

- **Increase monitoring power and redundancy: guarantee better stability**
- **Alternative flux determinations: $\gamma\gamma$, new end of line monitor, target, chamber**
- **Increase acceptance: allow even safer treatment for edge effects**
- **Increase statistics per energy point**

Aim at performing two separate scans, 8—10 weeks each

Additional material

Details on the event count N_2

Background subtraction using side-bands (bremsstrahlung, ~4%)

Correction relative variation +-1%, statistical uncertainty on $\delta N_2 \sim 0.3\%$

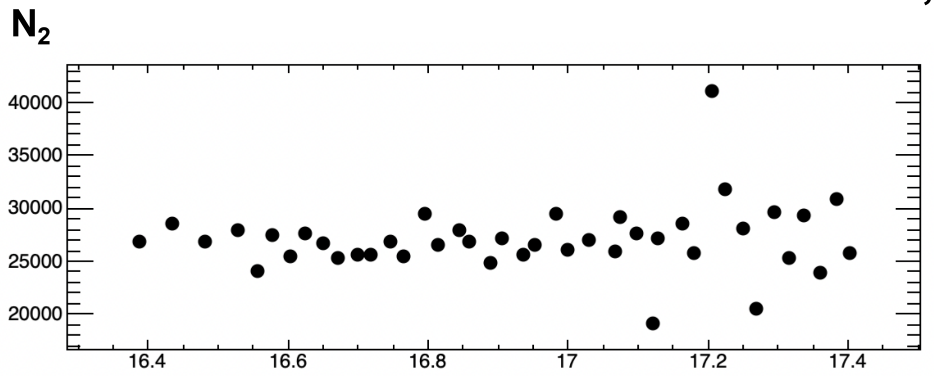

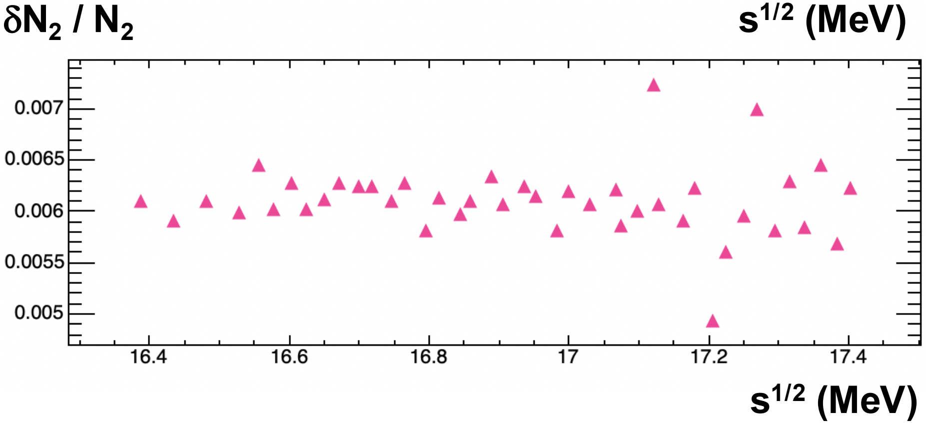

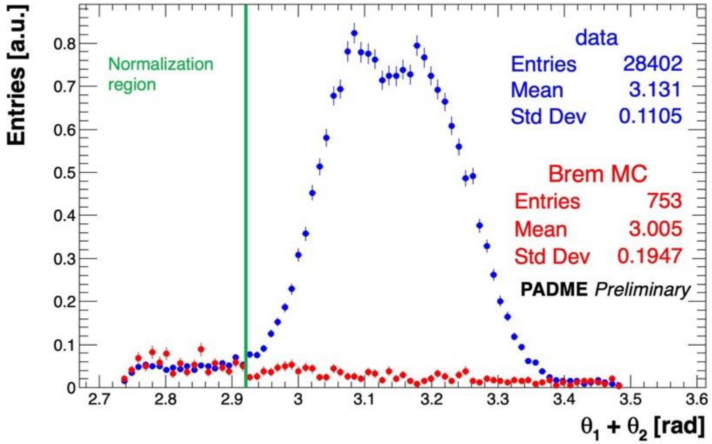

Shape of ee signal due to residual magnetic field (MNP CERN SPS type)

Fully modeled using MC + detailed map

Details on background: cut stability

Check if MC and data yields stable vs R_{min}, R_{max} (edge effects, leakage)

Vary R_{max} by +-2 E_{Cal} cells around nominal cut of 270 mm: 230 mm → 300 mm

Yield variation: -5%, +3%

Uncorrelated error 0.3%

R_{min} -1.5 D ($s^{1/2}$ = 16.4 MeV)
R_{min} -1.5 D ($s^{1/2}$ = 16.9 MeV)
R_{min} -1.5 D ($s^{1/2}$ = 17.5 MeV)

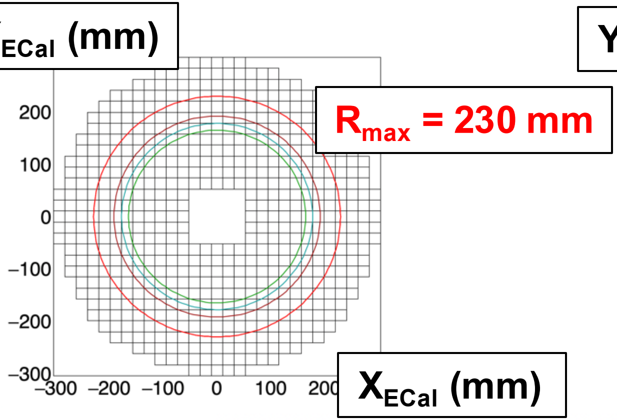

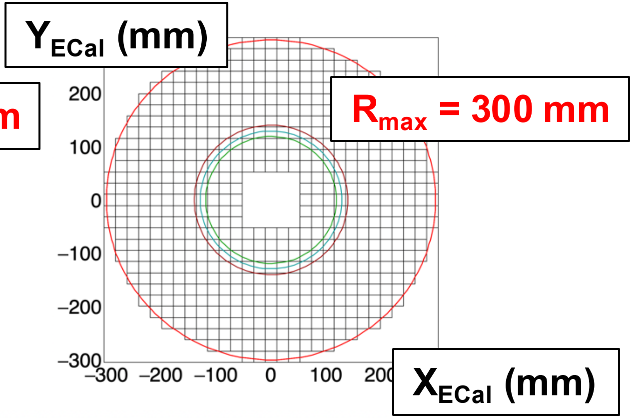

Stability is observed within a coverage band of **+-0.2%**, used as additional uncorrelated systematic error on B

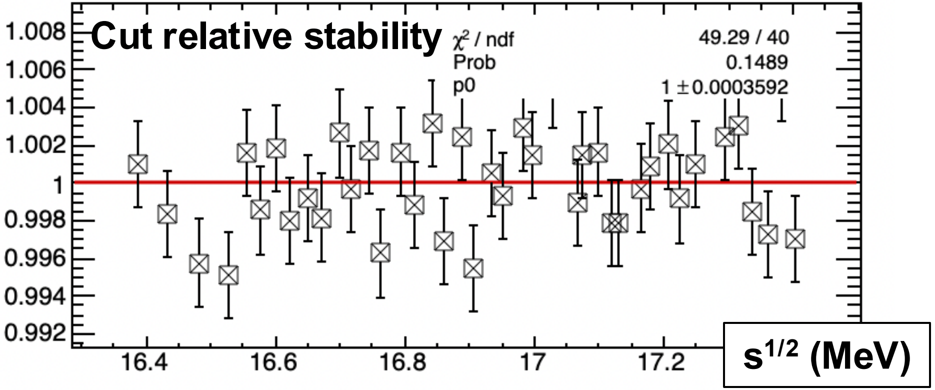

Details on background: acceptance variations

The selection makes use of the expected beam direction, from the spot measured at the diamond target and the center of gravity (COG) of 2 body final states at ECal

Systematic shifts in the COG position translate into acceptance systematic errors

Largest effect in y due to acceptance limitations (rectangular magnet bore)
Fractional variations range from 0.08% to 0.1% mm^{-1} for $s^{1/2}$ from 16.6 to 17.3 MeV

An error of 1 mm in the COG is a conservative estimate → systematic error < 0.1%

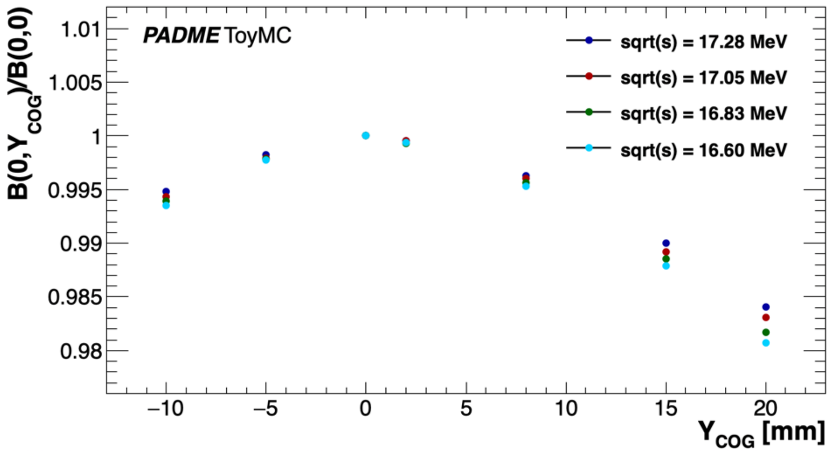

Details on background: cluster reconstruction

Tag and probe technique, the method-induced bias is 2.3(2)% and stable along the data set

Data/MC method efficiency stable along the data set and at the few per mil

Efficiency <Method /MC true>

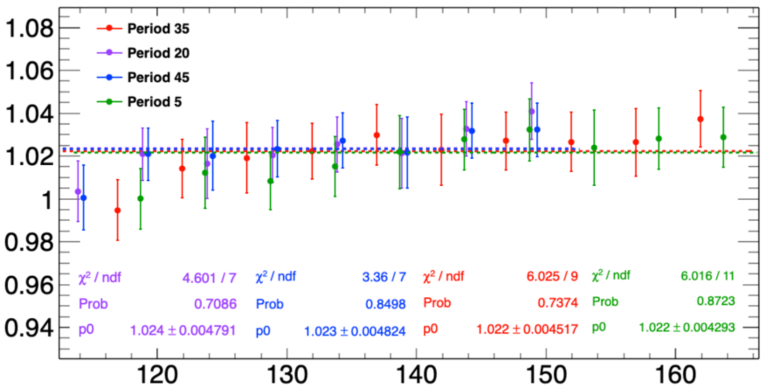

Expected cluster energy (MeV)

Efficiency Data/MC

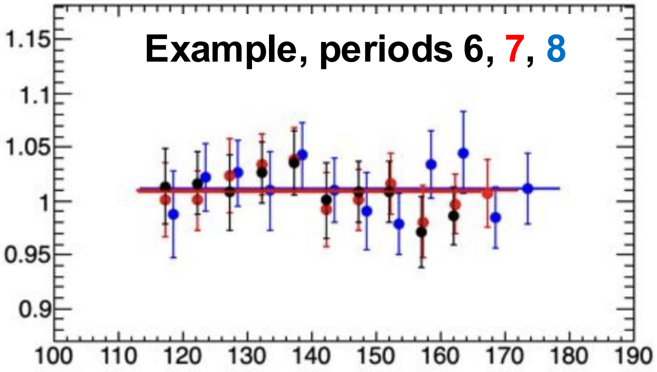

Expected cluster energy (MeV)

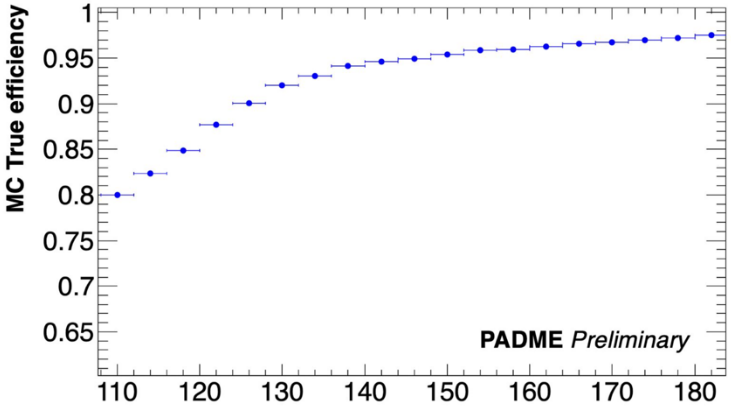

True energy (MeV)

Details on background: cluster reconstruction

Check of reconstruction efficiency:

Efficiency for data and MC evaluated using tag-and-probe technique
Statistical error dominated by background subtraction at tag level

Data/MC energy-flat, compatible with 1, error O(1%) per period

<Data/MC> vs period, P_{Fit}(const) ~ 20%

No correction applied per period, statistical-systematic error of 0.3%

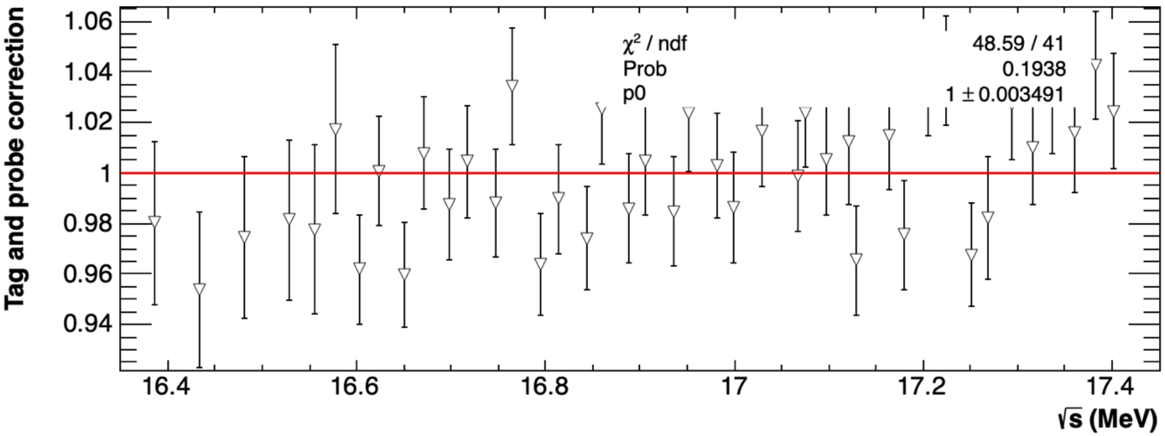

Leadglass PMT cathode limitations

(1) Cathode linearity

Parameters / Photocathode Materials	Spectral response (Peak wavelength) (nm)	Upper limit of linearity (Average current)
Ag-O-Cs	300 to1200 (800)	1 μA
Sb-Cs	up to 650 (440)	1 μA
Sb-Rb-Cs	up to 650 (420)	0.1 μA
Sb-K-Cs	up to 650 (420)	0.01 μA
Sb-Na-K	up to 650 (375)	10 μA
Sb-Na-K-Cs	up to 850 (420), up to 900 (600) extended red	1 μA
Ga-As (Cs)	up to 930 (300 to 700)	(∗) 1 μA
Ga-As-P (Cs)	up to 720 (580)	(∗) 1 μA
Cs-Te	up to 320 (210)	0.1 μA
Cs-I	up to 200 (140)	0.1 μA

(∗) Cathode sensitivity considerably degrades if this current is high.

Table 4-4: Photocathode materials and cathode linearity limits

Hamamatsu PMT handbook, section 4.3.2

What’s PADME – the detector: beam monitors

1.5 × 1.5 mm² spot at active, 100 μm diamond target: position, multiplicity

1 × 1 mm² pitch X,Y graphite strips [NIM A 162354 (2019)]

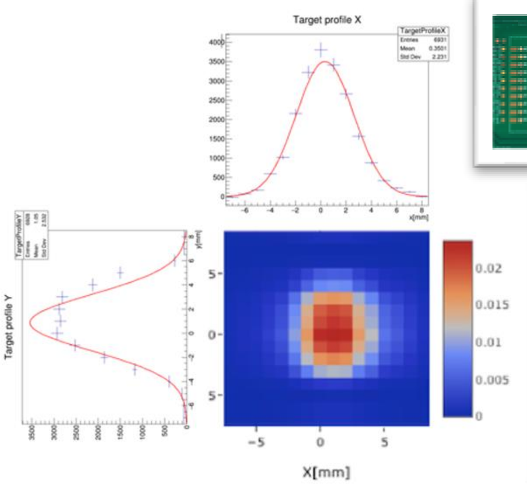

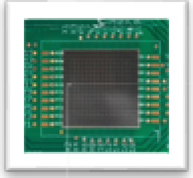

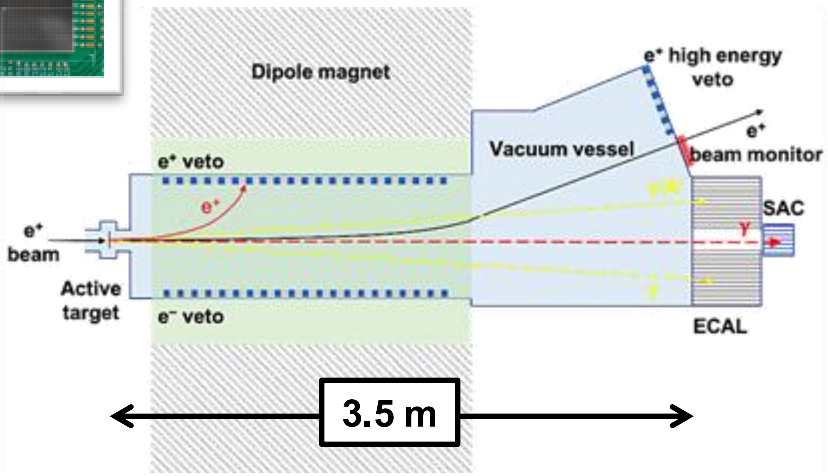

CERN MBP-S type dipole: 112×23 mm² gap, 70 cm long

Beam monitor (Si pixels, Timepix3) after bending: $\sigma_P/P_{beam} < 0.25\%$

What's PADME – the TDAQ concepts

Three trigger lines: Beam based, Cosmic ray, Random

Trigger and timing based on custom board [2020 IEEE NSS/MIC, doi: 10.1109/NSS/MIC42677.2020.9507995]

Most detectors acquired with Flash ADC's (CAEN V1742), O(10^3) ch's:

- **1 μs digitization time window**
- **1 V dynamic range, 12 bits**
- **sampling rates at 1, 2.5, 5 GS/s**

Level 0 acquisition with zero suppression, ×10 reduction → 200 KB / ev.
Level 1 for event merging and processing, output format ROOT based

First experiment goal (A' invisible search) required 10^{13} POT, O(80 TB)

Details on the flux N_{POT}: leakage correction

Loss from detailed MC vs vertical position checked against data in test beam

Very good data-MC agreement, correction 1.2%, systematic error 0.5%

Significant period-by-period variation of the correction: -4% to +2%

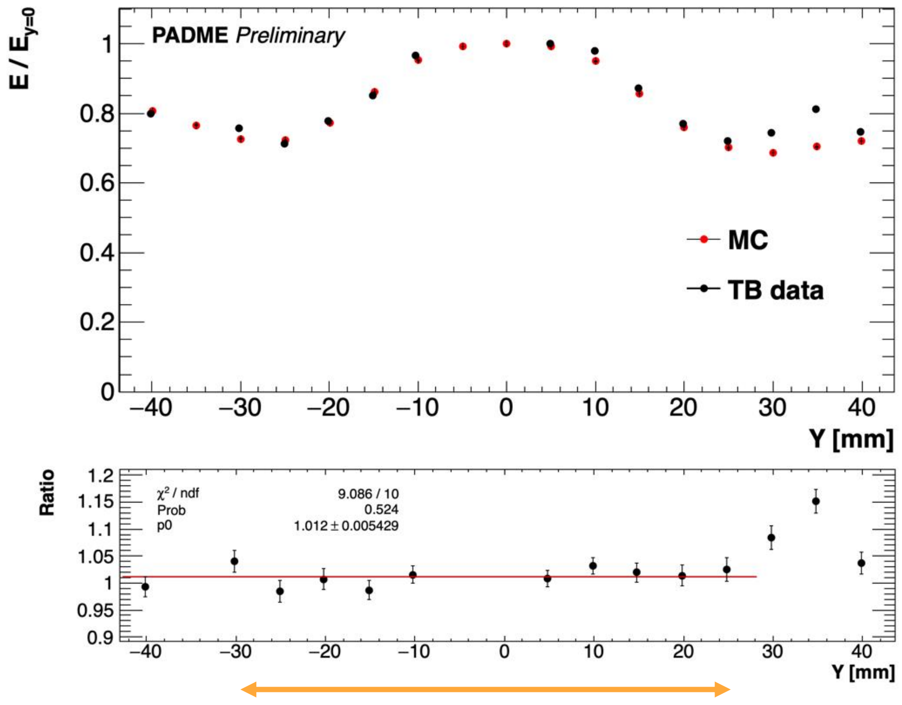

Region of interest

Relative leakage correction

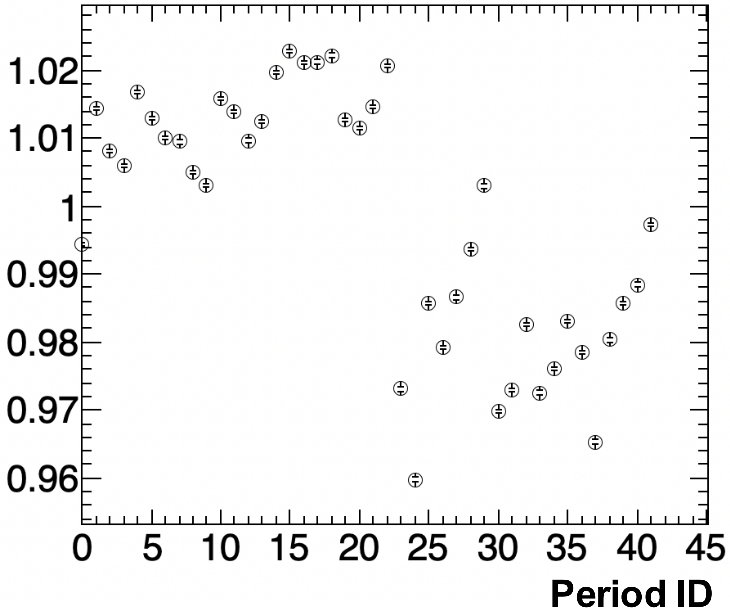

Details on the flux N_{POT}: ageing correction

The literature indicates possible changes in SF57 transparency for O(krad)

Estimate of Run-III dose: 2.5 krad

Estimated from 3 flux proxy observables: Qx target, <E_{Ecal}>, period multiplets

Leadglass yield decreases with relative POT slope of 0.097(7)

Constant term uncertainty of 0.3% added as scale error

Slope error included in POT uncertainty

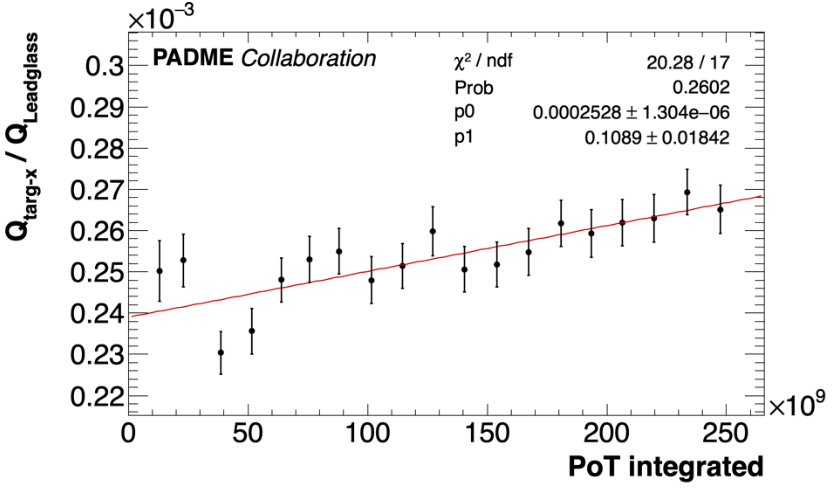

Relative ageing correction

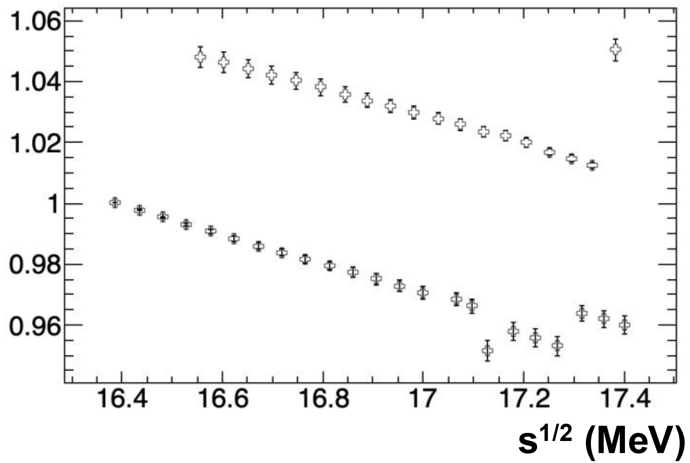

Details on the flux N_{POT}: ageing correction

The literature indicates possible changes in SF57 transparency for O(krad)

- **Estimate of Run-III dose: 2.5 krad**

Estimated from 3 flux proxy observables: Qx target, $\langle E_{Ecal} \rangle$, period multiplets

- **Leadglass yield decreases with relative POT slope of 0.097(7)**
- **Constant term uncertainty of 0.3% added as scale error**
- **Slope error included in POT uncertainty**

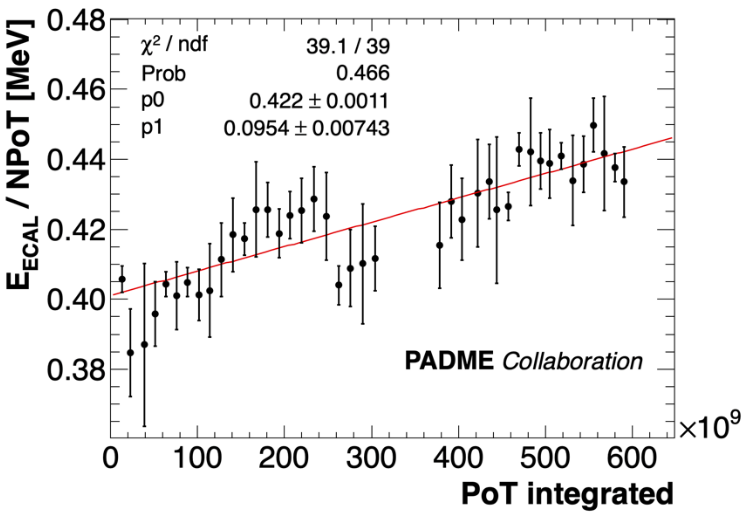

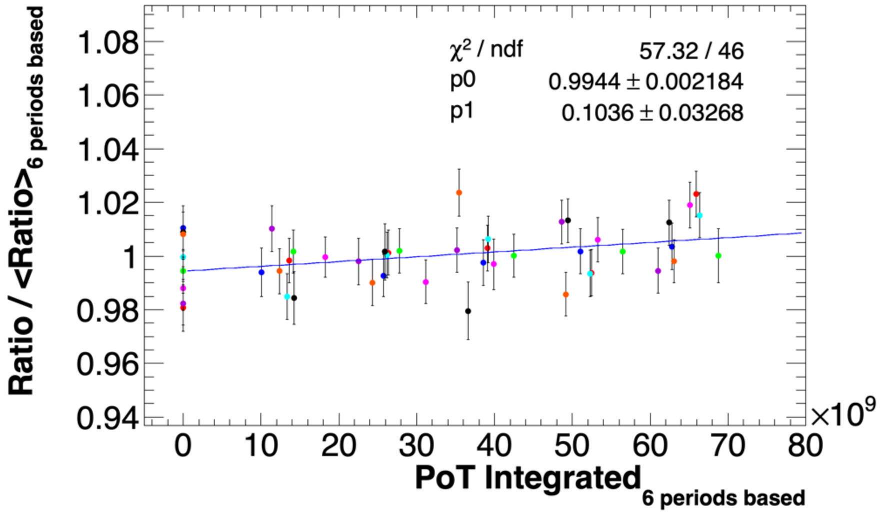

Measurement of $e^+e^- \rightarrow \gamma\gamma$: data set and concept

Using < 10% of Run II data, $N_{POT} = (3.97 \pm 0.16) \times 10^{11}$ positrons on target

- **Expect $N_{ee\rightarrow\gamma\gamma}$ ~0.5 M, statistical uncertainty < 1%**
- **Include various intensities, e^+ time profiles for systematic studies**
- **Evaluate efficiency corrections from MC + data**

Master formula:

$$\sigma_{e^+e^-\rightarrow\gamma\gamma} = \frac{N_{e^+e^-\rightarrow\gamma\gamma}}{N_{POT} \cdot n_{e/S} \cdot A_g \cdot A_{mig} \cdot \epsilon_{e^+e^-\rightarrow\gamma\gamma}}$$

N_{POT} from diamond active target

Uncertainty on e^- density $n_{e/S} = \rho N_A Z/A\ d$ depends on thickness d

Run #	NPOT [10^{10}]	e^+/bunch [10^3]	length [ns]
30369	8.2	27.0 ± 1.7	260
30386	2.8	19.0 ± 1.4	240
30547	7.1	31.5 ± 1.4	270
30553	2.8	35.8 ± 1.3	260
30563	6.0	26.8 ± 1.2	270
30617	6.1	27.3 ± 1.5	270
30624	6.6	29.5 ± 2.1	270
30654	No-target	~ 27	~ 270
30662	No-Target	~ 27	~ 270

$e^+e^- \rightarrow \gamma\gamma$: POT, target thickness

↩

N_{POT} from active target, uncertainty is 4%:

1. **Absolute calibration by comparing with lead-glass calorimeter fully contained from 5k to 35k e+/bunch**
2. **When focusing beam into 1-2 strips, non-linear effects observed**

$n_{e/S}$ from target thickness, uncertainty is 3.7% (i.e., ~3.7 μm)

1. **Measured after assembly with profilometer with 1 μm resolution as difference with respect to the supporting surface**
2. **Correction due to roughness (quoted as 3.2 μm by producer): compare precision mass and thickness measurements on similar diamond samples**

The blind unblinding procedure: details

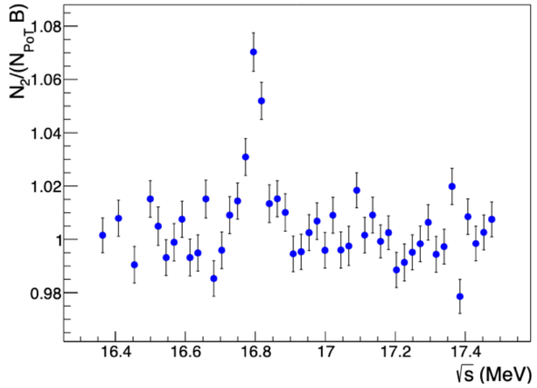

Constant term and slope of the optimized fit estimate the true values for K(s)

Results of the procedure ran on toy experiments with constant = 1, slope = 0

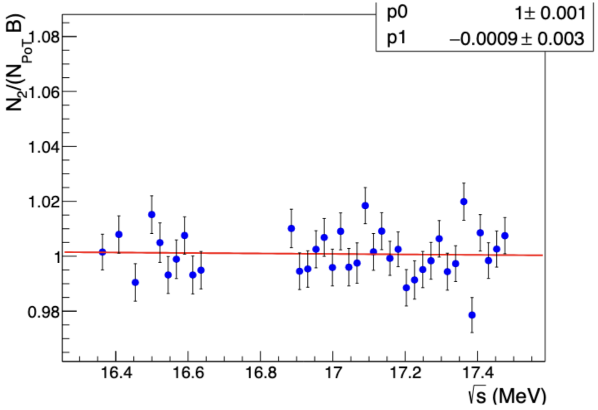

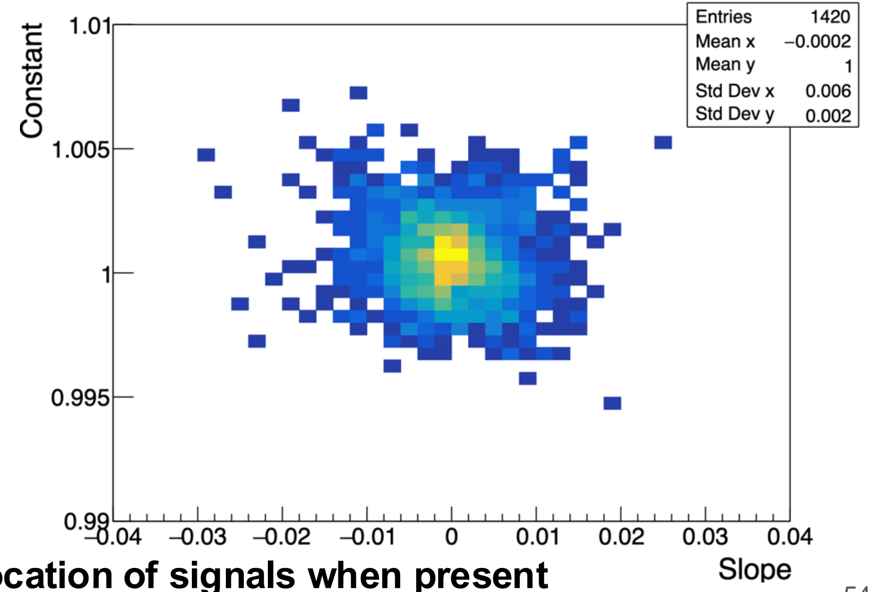

Moreover the procedure correctly finds the central location of signals when present

The PCL method

Using CLsb but clipping to the median every downward fluctuation of the limit

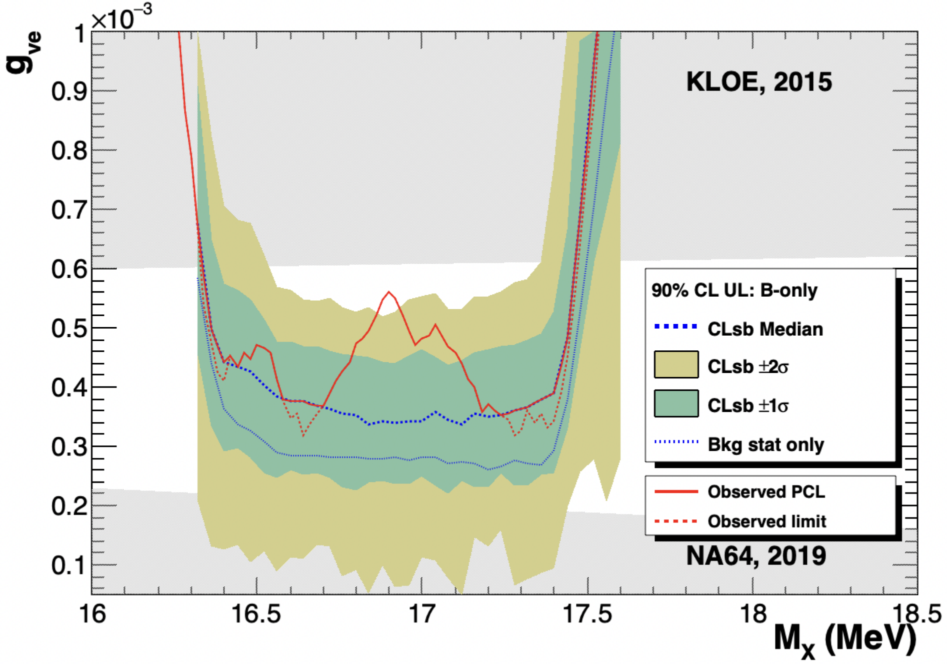

p-value

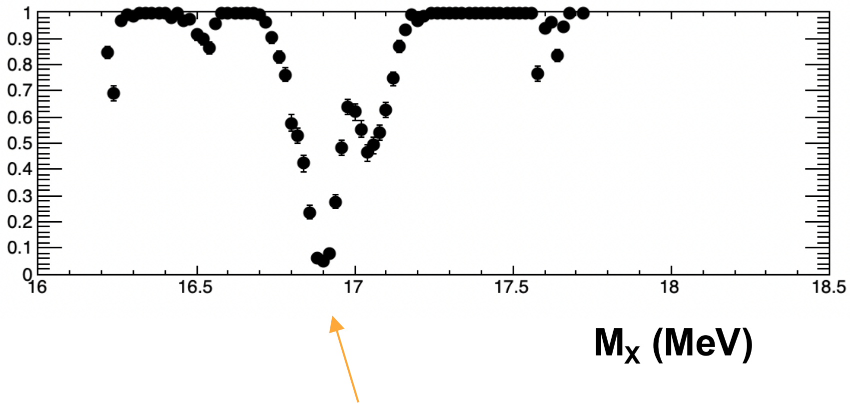

equivalent to (1.63 +- 0.13) σ

The p-value is only slightly affected, consistent with the coverage modifications of this method

The PADME ECal

The main detector for the signal selection [JINST 15 (2020) T10003]:

- 616 BGO crystals, 2.1 x 2.1 x 23 cm^3
- BGO covered with diffuse reflective TiO_2 paint + 50–100 μm black tedlar foils (optical isolation)

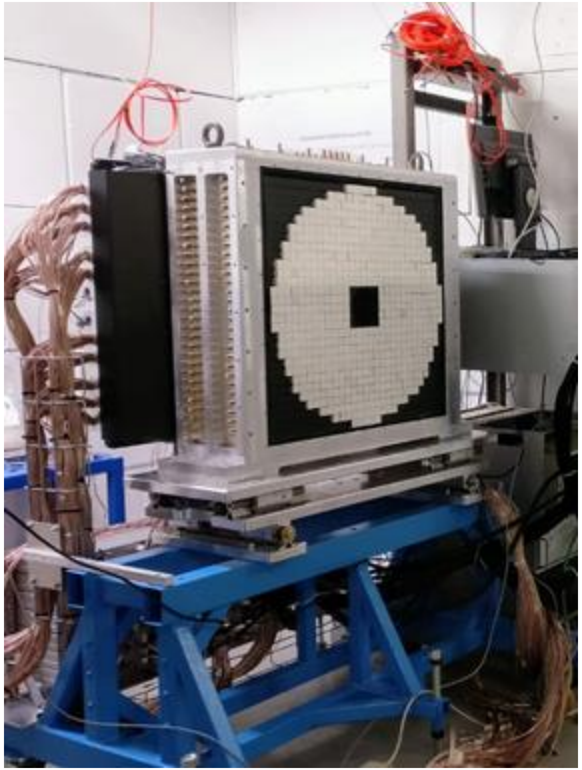

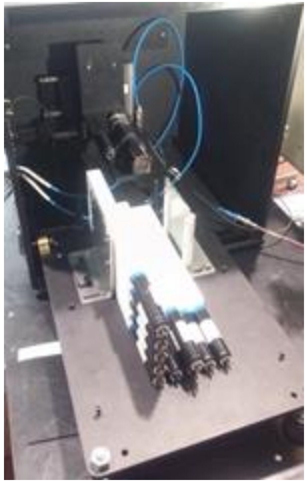

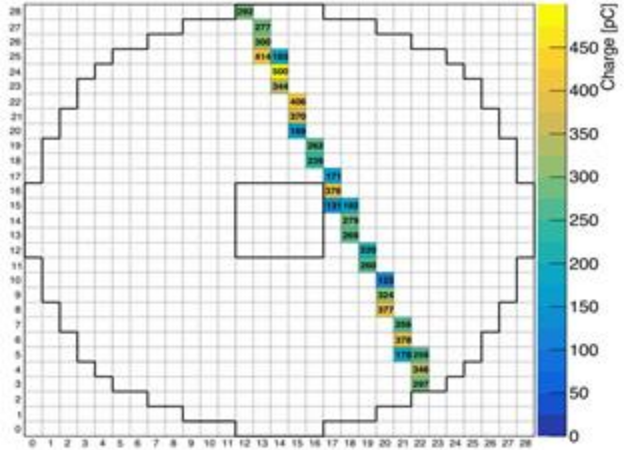

Calibration at several stages:

- BGO + PMT equalization with ^{22}Na source before construction
- Cosmic-ray calibration using the MPV of the spectrum
- Temperature monitoring + scale correction data driven

The PADME beam catcher calorimeter

The main detector for the flux determination [JHEP 08 (2024) 121]:

- SF57 block, reused from OPAL, tested for the NA62 LAV detector [JINST 12 (2017) 05, P05025]
- Several testing campaigns
  - A few positrons
  - O(2000) PoT - cross-calibration with the BTF FitPix

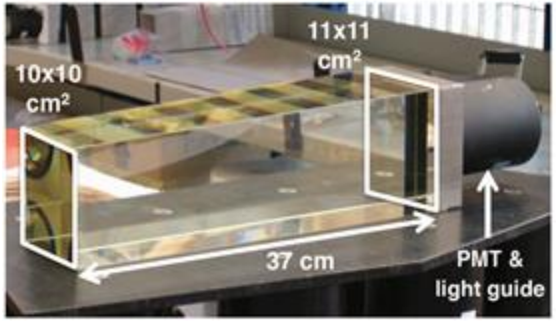

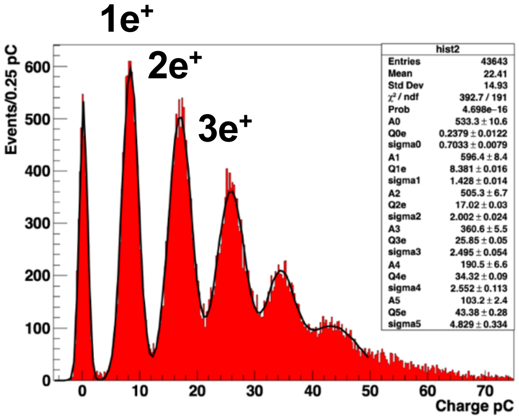

Figure 16. Single particle charge spectrum.

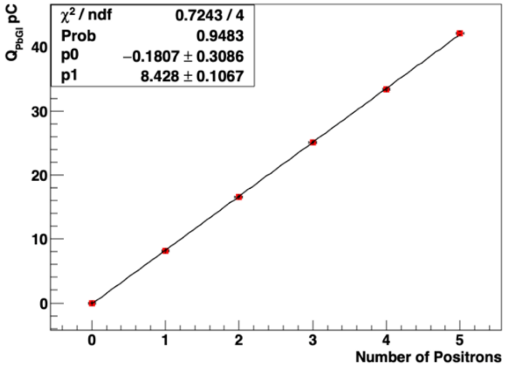

Figure 17. Fit to the single particle response.